To the Graduate Council:

I am submitting herewith a thesis written by Christopher Eugene Columber entitled "Structural Clay Tile Component Behavior." I have examined the final copy of this thesis for form and content and recommend that it be accepted in partial fulfillment of the requirements for the degree of Master of Science, with a major in Civil Engineering.

Richard M. Bennett

Dr. Richard M. Bennett, Major Professor

We have read this thesis and
recommend its acceptance:

Edwin G. Burdette

Accepted for the Council:

Associate Vice Chancellor
and Dean of the Graduate School

STATEMENT OF PERMISSION TO USE

In presenting this thesis in partial fulfillment of the requirements for a Master's degree at the University of Tennessee, Knoxville, I agree that the library shall make it available to borrowers under rules of the library. Brief quotations from this thesis are allowable without special permission, provided that accurate acknowledgement of the source is made.

Permission for extensive quotation from or reproduction of this thesis may be granted by my major professor, or in his absence, by the Head of Interlibrary Services when, in the opinion of either, the proposed use of the material is for scholarly purposes. Any copying or use of the material in this thesis for financial gain shall not be allowed without my written permission.

Signature Christopher E. Cole

Date April 27, 1994

DEDICATION

This thesis is dedicated to my mother, Mrs. Betty Joyce Columber, and to my late father, Mr. Jack Columber. Without their love, support, and sacrifices none of this would have been possible.

ACKNOWLEDGEMENTS

An undertaking such as this is not possible to complete alone, and I must express my gratitude to several people. First, I would like to thank my main professor, Dr. Richard M. Bennett. The opportunities he has provided me over the past three years have allowed me to achieve things I did not think possible. I would like to also thank my other committee members, Dr. Edwin G. Burdette and Dr. David Goodpasture. All three of these men exhibited both guidance and patience. I also want to thank Roger Flanagan and Martin Marietta Energy Systems for both their educational and economic assistance. Last, but certainly not least, I want to thank the people in the lab who worked on my thesis research sometimes harder than I did. This group includes Joele Fowler, George Barclay, Kurt Boyd, Jim Bernardi, and Archie W. Jordan. All of the people mentioned above made this possible.

ABSTRACT

The basic properties of structural clay tile walls were determined through component and composite testing of structural clay tile and mortar. The fundamental material parameters and strengths of clay tile coupons were determined through compression, tension, modulus of rupture and absorption tests. Mortar cylinders were tested in both compression and split cylinder fashion. Stress - strain curves for mortar under compression were determined.

Four miniature prisms were tested in compression. These prisms were made from two 8" x 12" x 12" structural clay tiles, using a stack bond with a 3/4" mortar joint. Stress - strain curves as well as material property values were obtained. These results were compared with previous tests on larger (2' x 4') prisms.

Twenty five bond wrench samples were tested. Two series of bond wrench samples were run. The first series (six tests) were fitted with LVDTs so that load - deflection curves as well as flexural strengths could be obtained. A shifting of the neutral axis towards the compression face was observed. The second series were made with different mortar types: type N masonry cement mortar, type S masonry cement mortar, type N portland cement lime (PCL) mortar, and type S PCL mortar. Type S mortar and portland cement lime mortar were found to improve the bond strength.

TABLE OF CONTENTS

CHAPTER PAGE

1. INTRODUCTION AND PURPOSE....1

2. TESTING PROCEDURES AND RESULTS OF CLAY TILE COUPONS..5

Introduction....5

Coupon Preparation and Testing....5

Compressive Test Results....11

Tensile Test Results....16

Modulus of Rupture Test Results....21

Absorption Test Results....22

3. TESTING PROCEDURES AND RESULTS OF MORTAR CYLINDERS..27

Introduction....27

Mortar Cylinder Preparation and Testing....27

Mortar Cylinder Test Results Under Monotonic Loading....29

Mortar Cylinder Test Results for Cyclic Loading....35

Test Results for Split Tensile Samples....40

Air Cure vs. Moist Cure Test Results....42

4. TESTING PROCEDURES AND RESULTS OF MINIATURE PRISMS..45

Introduction....45

Miniature Prism Preparation and Testing Procedures....45

Prism Strength Test Results....47

Comparisons with Other Test Results....55

5. TESTING PROCEDURES AND RESULTS OF BOND WRENCH SAMPLES.....58
Introduction.....58
Bond Wrench Samples Preparation and Testing....58
Bond Wrench Test Results.....63
Comparisons with Other Test Results.....72
6. CONCLUSIONS.....77
BIBLIOGRAPHY.....81
APPENDIX.....86
VITA.....91

LIST OF FIGURES

FIGURE		PAGE
1.1	Dimensions of 4" and 8" Structural Clay Wall Tile (Flanagan et al., 1993)	2
2.1.1	Modulus of Rupture Sample Loading	7
2.2.1	Stress-Strain Curves for Comp. Sample #1	12
2.2.2	Stress-Strain Curves for Comp. Sample #2	12
2.2.3	Stress-Strain Curves for Comp. Sample #3	13
2.2.4	Compressive Samples Test Results	13
2.2.5	Poisson's Ratio vs. Stress for Compressive Sample #1	14
2.2.6	Poisson's Ratio vs. Stress for Compressive Sample #2	14
2.2.7	Poisson's Ratio vs. Stress for Compressive Sample #3	15
2.3.1	Stress-Strain Curves for Tensile Sample #1	17
2.3.2	Stress-Strain Curves for Tensile Sample #2	17
2.3.3	Stress-Strain Curves for Tensile Sample #3	18
2.3.4	Tensile Samples Test Results	19
2.3.5	Poisson's Ratio vs. Stress - Tensile Sample #1 - 1st Test	20
2.3.6	Poisson's Ratio vs. Stress - Tensile Sample #1 - 2nd Test	20
2.4.1	Modulus of Rupture Samples Test Results	22
2.5.1	Absorption Samples Test Results	23

3.2.1 Full Stress-Strain Curves for Cyl. #1.....31
3.2.2 Partial Stress-Strain Curves for Cyl. #1.....31
3.2.3 Partial Stress-Strain Curves for Cyl. #2.....32
3.2.4 Mortar Cylinder Samples Test Results.....32
3.2.5 Poisson's Ratio vs. Stress for Cylinder #1.....34
3.2.6 Poisson's Ratio vs. Stress for Cylinder #2.....34
3.2.7 Mortar Cylinders Applied Loads and Stresses....35
3.3.1 Stress-Strain Curves - Cyl.#3 - Load Cyc. 1....37
3.3.2 Stress-Strain Curves - Cyl.#3 - Load Cyc. 2....37
3.3.3 Stress-Strain Curves - Cyl.#3 - Load Cyc. 3....38
3.3.4 Stress-Strain Curves for Cylinder #3 - Stress vs. Lateral Strains for all Load Cycles.....38
3.3.5 Stress-Strain Curves for Cylinder #3 - Stress vs. Longitudinal Strains for all Load Cycles..39
3.3.6 Reload Modulus Calculation Results.....40
3.4.1 Split Tensile Test Results.....41
3.5.1 Air Cured vs. Moist Cured Comparisons.....43
4.2.1 Stress-Strain Curves for Miniature Prism #1....48
4.2.2 Stress-Strain Curves for Miniature Prism #2....48
4.2.3 Stress-Strain Curves for Miniature Prism #3....49
4.2.4 Stress-Strain Curves for Miniature Prism #4....49
4.2.5 Prism Typical First Crack Patterns.....51
4.2.6 Miniature Prisms Test Results.....53
4.3.1 Comparison of Prism Results.....56
5.1.1 Bond Wrench 3 View Drawing.....60
5.1.2 Bond Wrench Test Apparatus.....60

5.2.1 Load Deflection Curves for Sample #2.....64
5.2.2 Load Deflection Curves for Sample #3.....64
5.2.3 Load Deflection Curves for Sample #4.....65
5.2.4 Load Deflection Curves for Sample #5.....65
5.2.5 Flexural Strengths of First Set of Samples.....68
5.2.6 Flexural Strengths of Second Set of Samples....69
5.2.7 Comparison of Mortar Cube Strengths.....71
5.3.1 Comparison of Different Bond Wrench Tests.....73
A.1 Miniature Prism Test Apparatus.....87
A.2 Miniature Prism Web Crack Pattern.....87
A.3 Mini Prism Faceshell Failure Pattern.....88
A.4 Mini Prism Explosive Failure Pattern.....88
A.5 Bond Wrench Test Apparatus.....89
A.6 Bond Wrench Failure Pattern.....89
A.7 Bond Wrench Failure Pattern (Close-up).....90
A.8 Bond Wrench Samples Mortar Joints.....90

Chapter 1

INTRODUCTION AND PURPOSE

Since 1991, The University of Tennessee has, under contract and with the cooperation of Martin Marietta Energy Systems, conducted a research program on the behavior of masonry infilled frames subjected to both in-plane and out-of-plane loading. As part of this program, unit tile tests were conducted, infilled frames and masonry prisms were tested, and other supporting tests were conducted. However, so that a better understanding of the interaction of the hollow clay tile units and the mortar could be achieved, a need to determine the basic material properties of both the clay tile material and the mortar arose.

The purpose of this thesis is both to describe the tests which were conducted to achieve the understanding of the basic materials and also to report the results of these tests. These tests included clay tile coupon tests, mortar cylinder tests, miniature prism tests, and bond wrench tests.

Structural clay tile has been manufactured in the U.S. for over a century. This tile is made of clay, water, and other chemical additives (Flanagan et al., 1993). The clay is mixed with the water and other additives, shaped, and then the unit is fired. Structural clay tile is distinguished by hollow units having parallel cores and thin

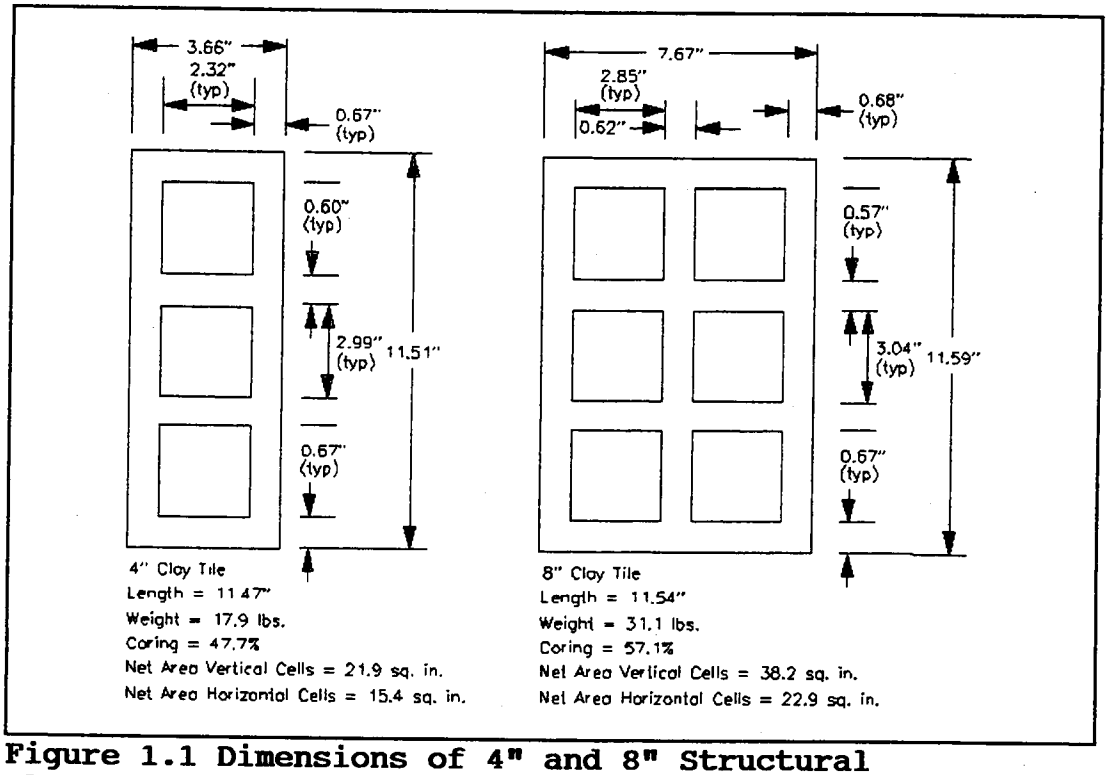


Figure 1.1 Dimensions of 4" and 8" Structural Clay Wall Tile (Flanagan et al., 1993)

webs and faceshells (Flanagan et al., 1993). The tile is available in different sizes, with the main sizes nominally 12 inches high by 12 inches long, in both 8 inch and 4 inch thicknesses. A drawing of the tiles with dimensions is shown in figure 1.1. ASTM C34 is the specification for structural clay tile, and these specifications have not significantly changed since 1927.

The clay tile coupons were solid pieces cut from clay tile material; a total of twenty five coupons were tested. Of these twenty five, there were three tensile coupons, three modulus of rupture coupons, four compressive coupons, and fifteen absorption coupons. The modulus of rupture

coupons were tested using third point loading. The tensile and compressive coupons had bidirectional strain gages attached, which allowed for both the construction of stress - strain curves and the determination of some material properties. All of the tile coupons were loaded monotonically to failure. The absorption coupons were tested according to ASTM standards. These tests were conducted in order to determine if the structural clay tile should be wetted prior to placement.

The mortar cylinders were all made from type N masonry cement mortar and were standard 2 inch diameter by 4 inch high samples. A total of eighteen cylinders were tested, with twelve cylinders tested in compression and six in split cylinder tension. Of the twelve compressive cylinders, three were fitted with bidirectional strain gages. As with the clay tile coupons, stress - strain curves and material properties were determined. A mixture of both monotonic and cyclic loading to failure was performed. The six split cylinder tests were tested according to ASTM standards.

The miniature prisms were constructed out of two 8" x 12" x 12" structural clay tiles using a stack bond and a 3/4" thick type N masonry cement mortar joint. These tests were carried out both to investigate the interaction aspect of the clay tile and mortar and also to compare the ultimate strength results with other tests. A total of four prisms were built, strapped together, and then capped and loaded in

a cyclic fashion to failure. Linear variable displacement transducers were attached over the mortar joints so that stress - strain curves and material properties could be determined.

Finally, two sets of bond wrench tests were performed. All of the bond wrench samples were constructed from two structural clay tile using a stack bond and a 3/4" thick mortar joint. In the first set, six samples were tested with both load - deflection curves plotted and flexural strengths found. In the second set, a total of twenty samples were laid up. Of these twenty samples, five each were constructed of type N masonry cement mortar, type S masonry cement mortar, type N portland cement lime (PCL) mortar, and type S PCL mortar. These tests were undertaken both to determine the effect of mortar type and strength on the bond strength and also to compare the results with previous tests.

This thesis is divided into four major sections, with each section describing both the testing procedures and the results of the four major test groups previously listed. The first section covers the tile coupon tests, the second the mortar cylinder tests, the third the miniature prism tests, and finally, the fourth the bond wrench tests. The third and fourth sections compare the obtained results to previous tests as well.

Chapter 2

TESTING PROCEDURES AND RESULTS OF CLAY TILE COUPONS

Introduction

The following sections cover the coupon testing which was performed. These "coupons" were small pieces of tile which were cut from whole structural clay tiles. The main reason for performing tests on these coupons was to find the properties of the clay tile material itself. Previous tests were performed on the clay tiles as unit tiles, in which a single unit of structural clay tile was subjected to a variety of tests. While this testing was very beneficial and provided needed results, the clay tile performed as a unit, with the voids interacting with the solid portion of the structural clay tile. With coupon testing, only solid material specimens of the clay tile were tested. A total of twenty five coupons were tested, with three tensile coupons, three modulus of rupture coupons, four compressive coupons, and fifteen absorption coupons.

2.1 Coupon Preparation and Testing

The coupons were of three main types. First, pieces of tile were cut in an approximately 2.25" x 12" size from the face shells. Three of this size were tested as tensile samples, in which the 12" length was needed in order to grip the sample in the jaws of the testing machine. Three of

this size were also tested as modulus of rupture samples, and an additional ten were tested as absorption samples. Secondly, an additional five of the same size were cut from the webs of the tiles. These five were used as absorption samples, and were cut in accordance with the sampling requirements of ASTM C67 7.2.2, the specification used for the absorption testing. Third, three compressive coupons were cut from material in the face shells. These compressive coupons were approximately 2.25" X 3". The shorter height of the compressive sample was needed to prevent buckling from affecting the results.

After the coupons were cut, the tensile, compressive, and modulus of rupture coupons were allowed to dry for approximately 24 hours. Following this drying period, the approximate center of the tensile and compressive samples were marked and MBond 200 epoxy was applied on both sides of these coupons. After allowing approximately 48 hours for the epoxy to dry, strain gages were applied to the coupons, with MBond 200 epoxy. These strain gages had two gage patterns such that both lateral and longitudinal strains could be obtained.

After the strain gages were attached, the tensile, compressive, and modulus of rupture samples were moved to the testing room and separated into their respective groups. The compressive coupons were then capped with sulfur compound so that a uniform bearing surface was obtained for

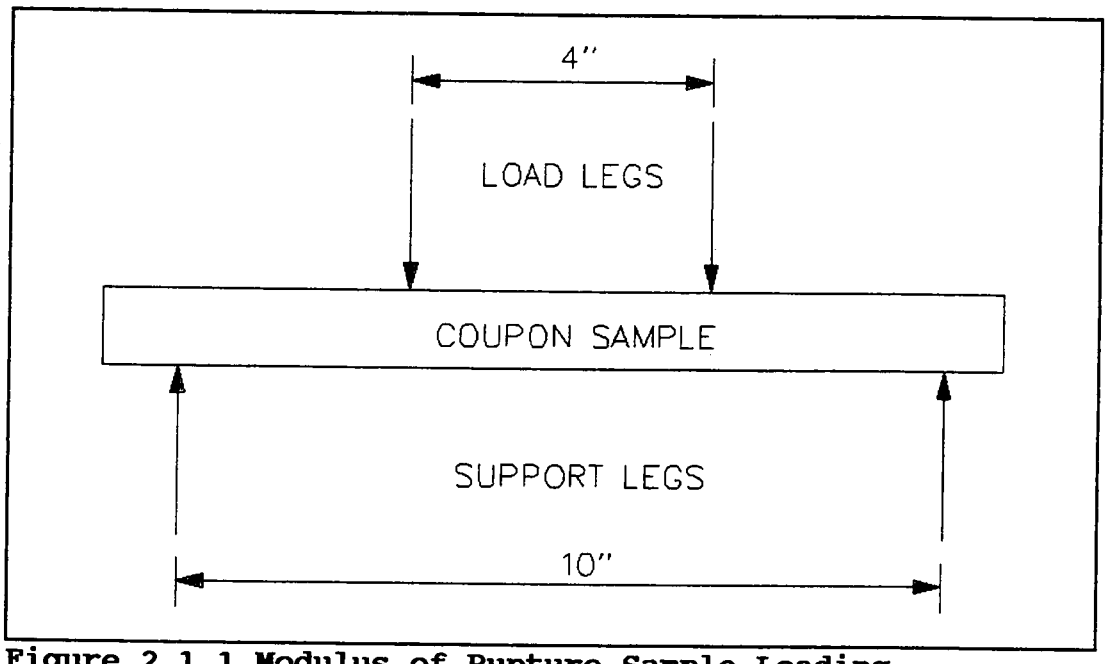


Figure 2.1.1 Modulus of Rupture Sample Loading

testing. The machine used for testing the coupons was a Tinius-Olsen Universal Testing machine with a 120,000 lb. capacity. This machine has three load ranges which are as follows: 1) 0 to 6,000 lbs. with graduations of 10 lbs. 2) 0 to 60,000 lbs. with graduations of 100 lbs. 3) 0 to 120,000 lbs. with graduations of 200 lbs. Depending on the test being performed, the machine was used in different load ranges.

As shown in figure 2.1.1, the modulus of rupture samples were loaded utilizing third point loading. These samples were put into the testing machine and loaded on the lowest range (0 to 6,000 lbs. with 10 lb. increments) until failure. The loading rate was kept under 1,000 lbs/minute. After failure, the ultimate load was recorded and the

sample's failure area was measured and recorded.

Testing of both the compressive and tensile coupons involved the set-up and use of a central data acquisition system. This system was an IBM PS/2 mated via an IEEE 488 interface with a Megadac 3008 data collection system. Load and strain readings were recorded on this system. The sampling rate was 10 samples per second. The strain gages were connected to a STB 884/SCV terminal block. This terminal block was connected to the Megadac via a 32 pin data cable.

Before testing, the compressive coupons had their bearing areas measured, as the cap applied to the coupons would make this impossible. The compressive coupons were then capped, as described earlier, and the strain gages were wired into the terminal block. Following this, the coupons were placed into the testing machine and loaded until failure. The loading rate was kept under 2,000 lbs./minute, with load levels recorded on the data acquisition every 500 pounds. The data collection recorded 4 strain readings as follows, front lateral strain, back lateral strain, front longitudinal strain, and back longitudinal strain, as well as the load levels. The sampling rate, as stated earlier, was 10 samples per second. The load levels were recorded by use of a "doorbell" device. This "doorbell" simply input an electrical surge or "spike" into the terminal block. This "spike" was recorded on the data collection system, and when

the data were later reduced these spikes were converted into load readings.

The tensile samples did not have to be capped, so the strain gages were wired into the terminal blocks and testing proceeded. These samples were loaded in tension until failure. To reduce stress concentrations, a rubber pad was placed between the specimen and testing machine jaws. The samples were held in place until 20 or 30 pounds of tension were applied to prevent the sample from slipping out of the clamp. The sample was then loaded in tension until failure, with load levels taken every 50 pounds. Each tensile sample was tested at least twice, with one sample being tested 4 times. This was possible because of the failure pattern exhibited by these samples. In every test, except one, the sample failed in the clamps. This was probably due to a combination of several factors, including high local stress concentrations, the irregular face of the samples being gripped by the clamps, and possible slipping and regripping. With respect to the data collection, the tensile samples were fairly similar to the compressive samples. The sampling rate was the same, with the same strain readings and load levels being recorded.

The absorption samples were placed in an oven kept at a temperature of 110 to 115°C for a period of not less than 24 hours and until two consecutive weighings 2 hours apart resulted in a weight loss of less than 0.2%. After this

requirement was met, the samples were allowed to cool for at least 4 hours, until they reached room temperature.

The samples were then weighed and this weight was recorded as the initial weight. The samples were then placed into a bath of water kept at 15.5 to 30°C. The samples were kept in this bath for 5 hours, at which point they were withdrawn from the water, had the excess surface moisture dried off, and weighed again. This weight was recorded as the 5 hour submersion weight. The samples were placed back into the bath and kept until 24 hours had passed since they were first placed into the bath. Once again, the samples were removed from the bath, had excess surface moisture removed, and were weighed. This weight was recorded as the 24 hour submersion weight.

After the samples had soaked in room temperature water for a period of 24 hours, they were then subjected to either a 1 or 5 hour boil test. This test was performed by placing the samples into the bath and then bringing the water to boiling. Once the water was boiling, the samples were boiled for a period of either 1 or 5 hours. Following the specified boil time, the samples were allowed to cool in the bath and were once again weighed. These weights were recorded as the 1 or 5 hour boiling weight.

2.2 Compressive Test Results

The results from the compressive tests were used in two main ways. First, the raw data were plotted to obtain stress - strain curves as seen in figures 2.2.1, 2.2.2, and 2.2.3. Second, the data was used to find material properties such as the modulus of elasticity, E, and Poisson's ratio.

The stress - strain curves obtained from the compressive coupons are shown in figures 2.2.1, 2.2.2, and 2.2.3. These curves show a fairly linear behavior up to approximately 60% of the ultimate stress. The modulus of elasticity, E, was calculated by utilizing linear regression on the stress - strain curve from 0 to 50% of the ultimate stress. The values obtained for E are tabulated in figure 2.2.4.

The other material property calculated for the compressive coupons was Poisson's ratio. Poisson's ratio, ν, is calculated by the following formula,

$$\nu = -\frac{lateral\ \epsilon}{axial\ \epsilon}$$

Stress is plotted against Poisson's ratio in figures 2.2.5, 2.2.6, and 2.2.7. As can be seen in these plots, the value of Poisson's ratio increases with higher levels of stress. It is possible that internal coupon damage is responsible for this increase in Poisson's ratio.

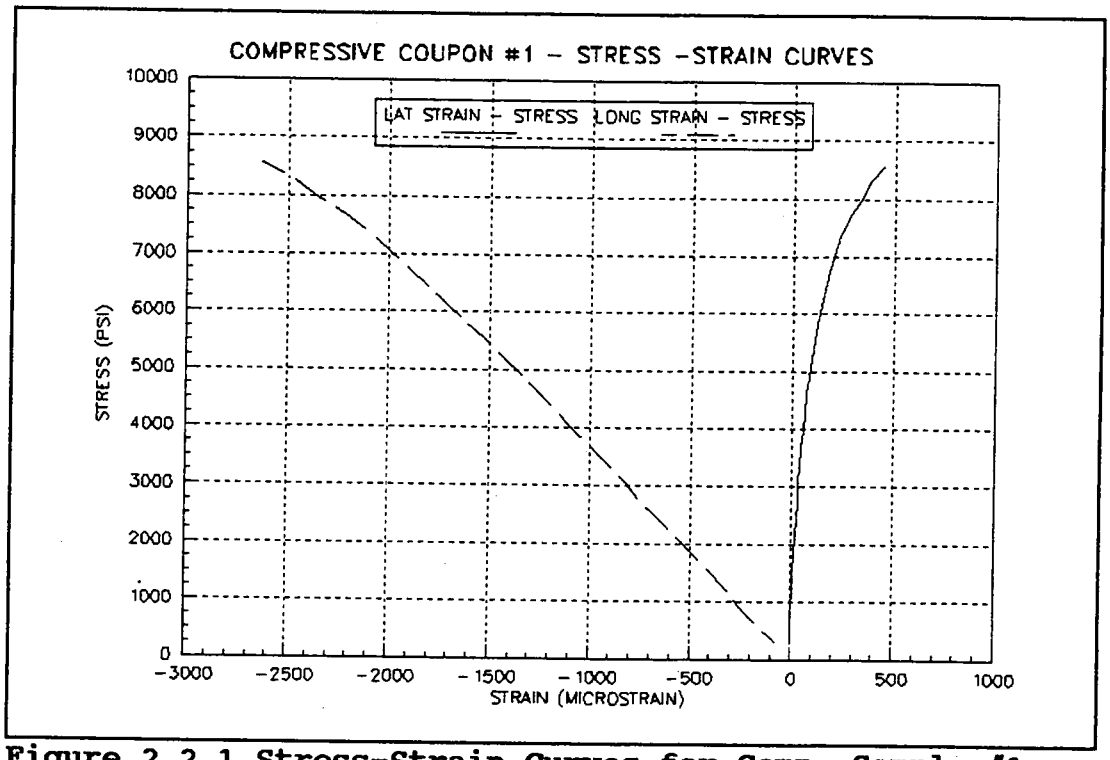


Figure 2.2.1 Stress-Strain Curves for Comp. Sample #1

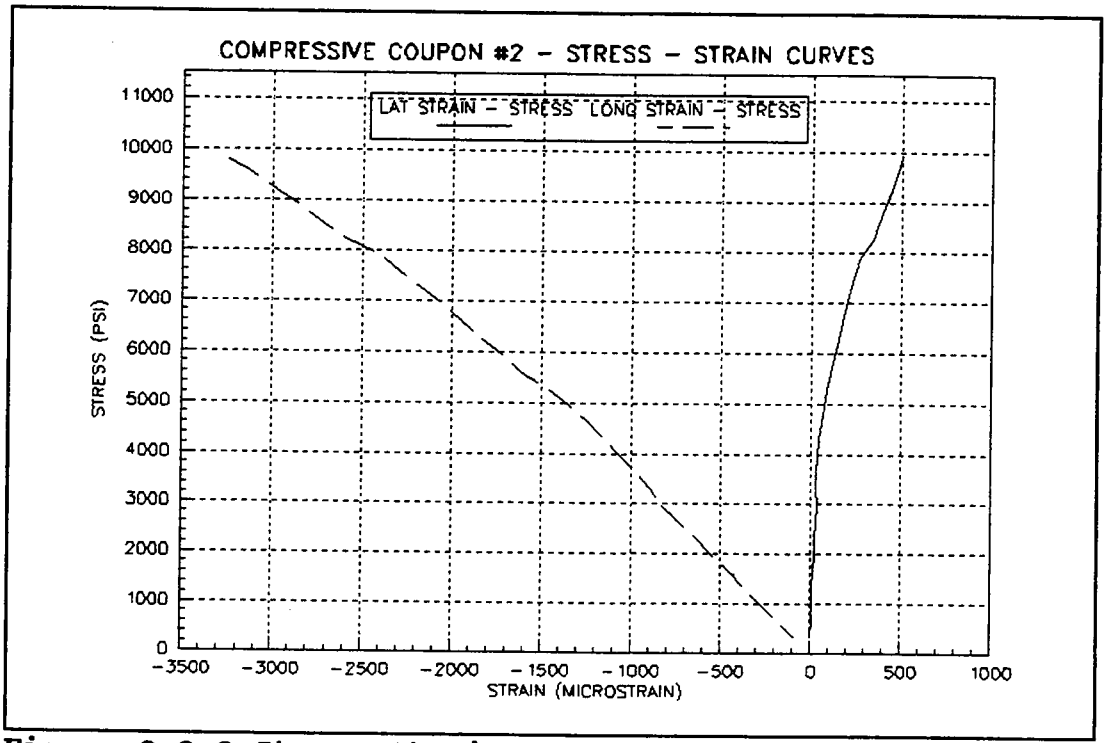


Figure 2.2.2 Stress-Strain Curves for Comp. Sample #2

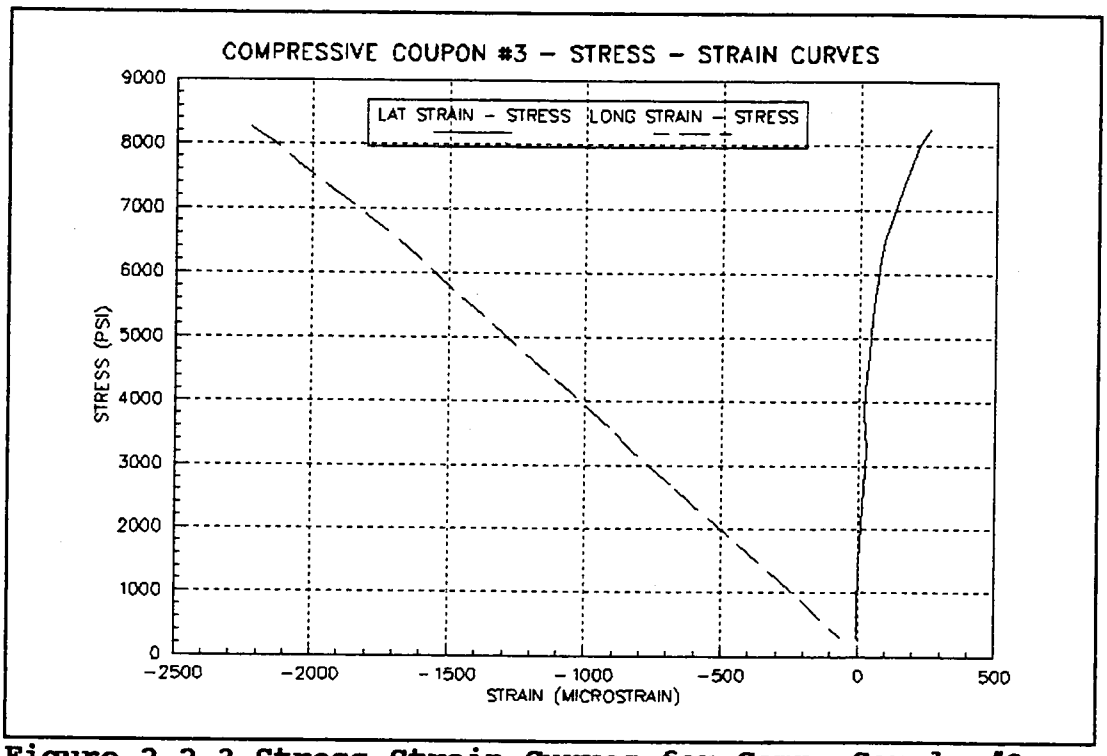


Figure 2.2.3 Stress-Strain Curves for Comp. Sample #3

Compressive Sample #	Compressive Strength, psi	Modulus of Elasticity, psi	Poisson's Ratio
#1	8900	3,670,000	0.0518
#2	10000	3,750,000	0.0527
#3	8550	3,860,000	0.0245
Averages	9150	3,760,000	0.0430
C.O.V.	6.7%	2.1%	30.4%

C.O.V. = Coefficient of Variation

Figure 2.2.4 Compressive Samples Test Results

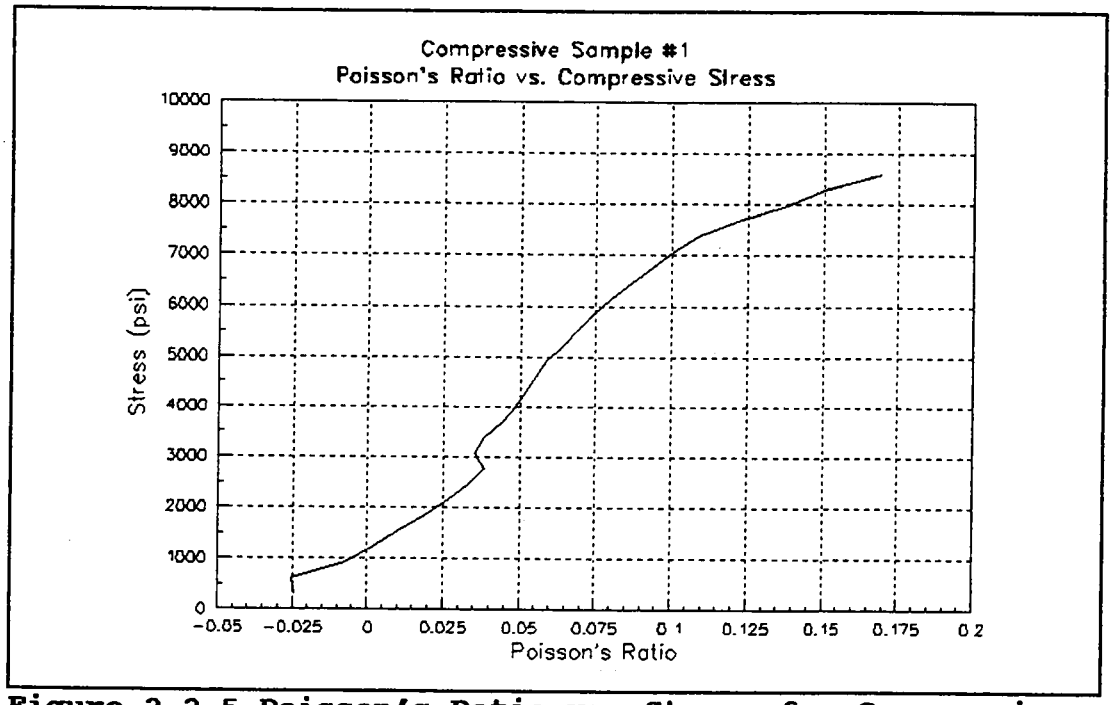


Figure 2.2.5 Poisson's Ratio vs. Stress for Compressive Sample #1

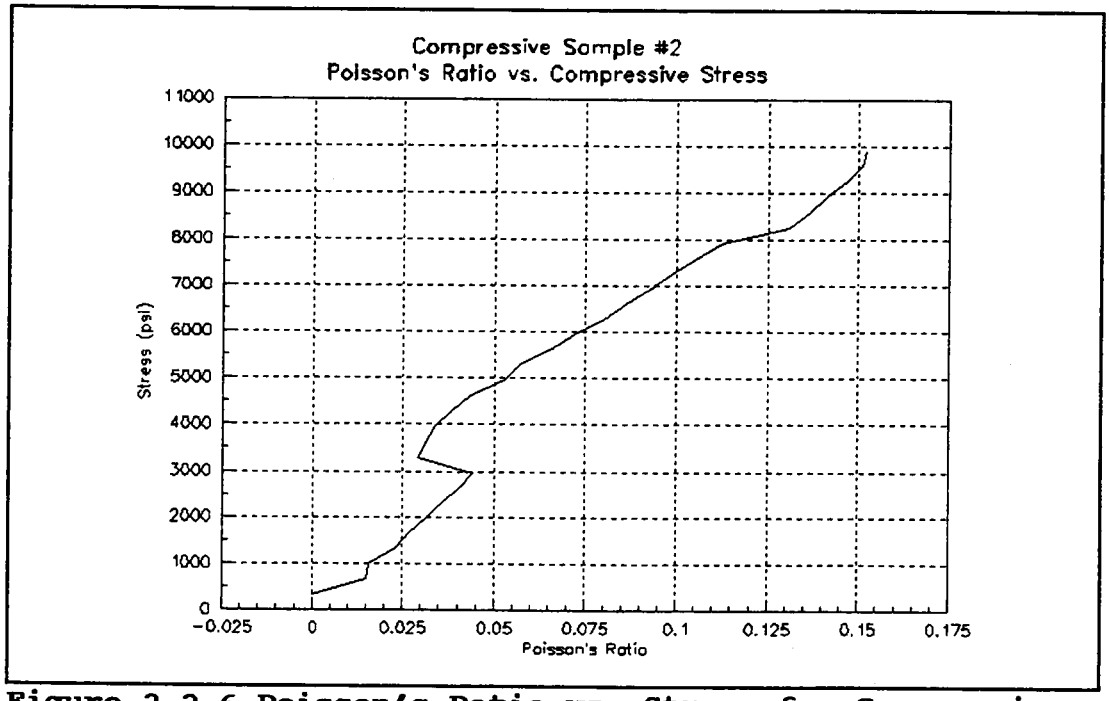


Figure 2.2.6 Poisson's Ratio vs. Stress for Compressive Sample #2

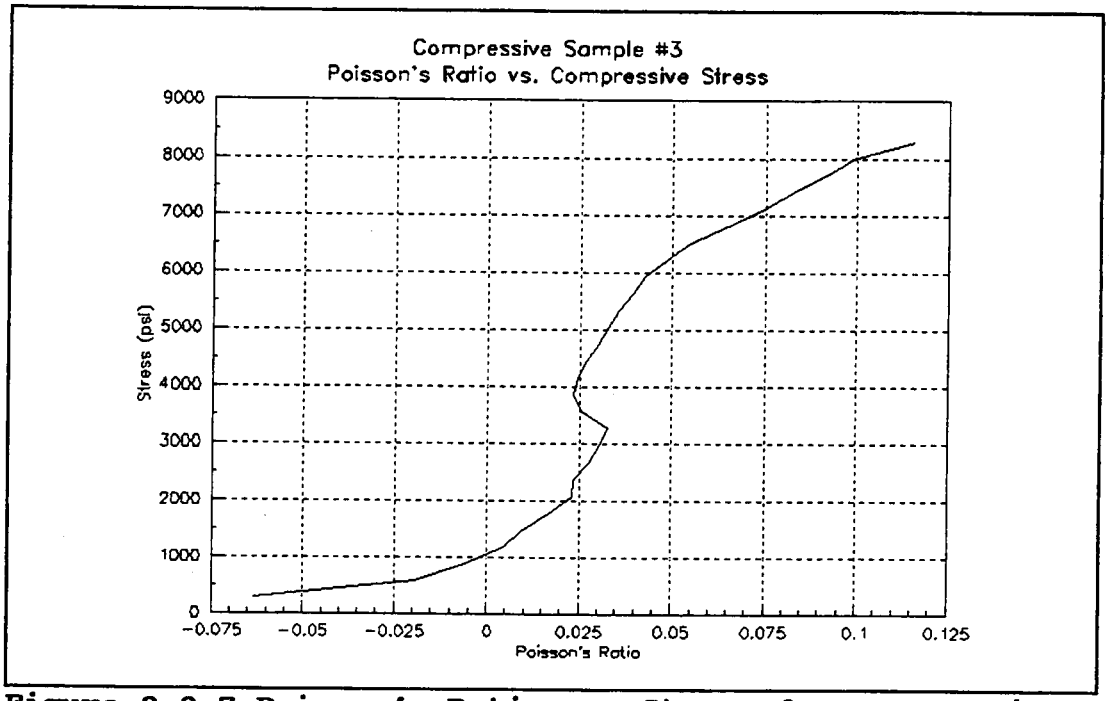


Figure 2.2.7 Poisson's Ratio vs. Stress for Compressive Sample #3

The values of Poisson's ratio at 50% of the ultimate stress are presented in figure 2.2.4. In addition to the individual values of Poisson's ratio in figure 2.2.4, the average value of all three compressive samples are given. Poisson suggested a value of approximately 0.25 for isotropic materials (Gere and Timoshenko, 1990). The values obtained are considerably lower than this. Poisson's ratio for concrete is approximately 0.1 to 0.2 (Mehta, 1986). Plummer (1962) suggested that Poisson's ratio for tile would probably fall in a range of 0.05 to 0.10, which is close to the results obtained.

2.3 Tensile Test Results

The data obtained from the tensile samples were used in approximately the same manner as the compressive sample data. The raw data were used to plot stress - strain curves, and these curves were used to find material properties.

The stress - strain curves for the tensile samples, for the most part, display linear behavior practically up to ultimate stress. This is probably because the clay tile material, much like concrete, is weak in tension, and deforms nonlinearly very little before failure. Also factors such as high local stress concentrations, irregular faces of the tile being gripped by the rigid jaws of the testing machine, and possible slipping and regripping could have caused premature failure.

These stress - strain curves are presented in figures 2.3.1, 2.3.2, and 2.3.3, representing the first sample - first test, second sample - first test, and the third sample - second test tensile tests. These samples and tests were chosen because they showed the most consistent results, and were the tensile samples which sustained the highest stress levels. The other tests on the tensile samples displayed erratic behavior, most likely due to slipping and breaking in the testing machine jaws, as well as internal damage inflicted on the samples by earlier tests. Also, with the exception of the third sample, the stress - strain curves

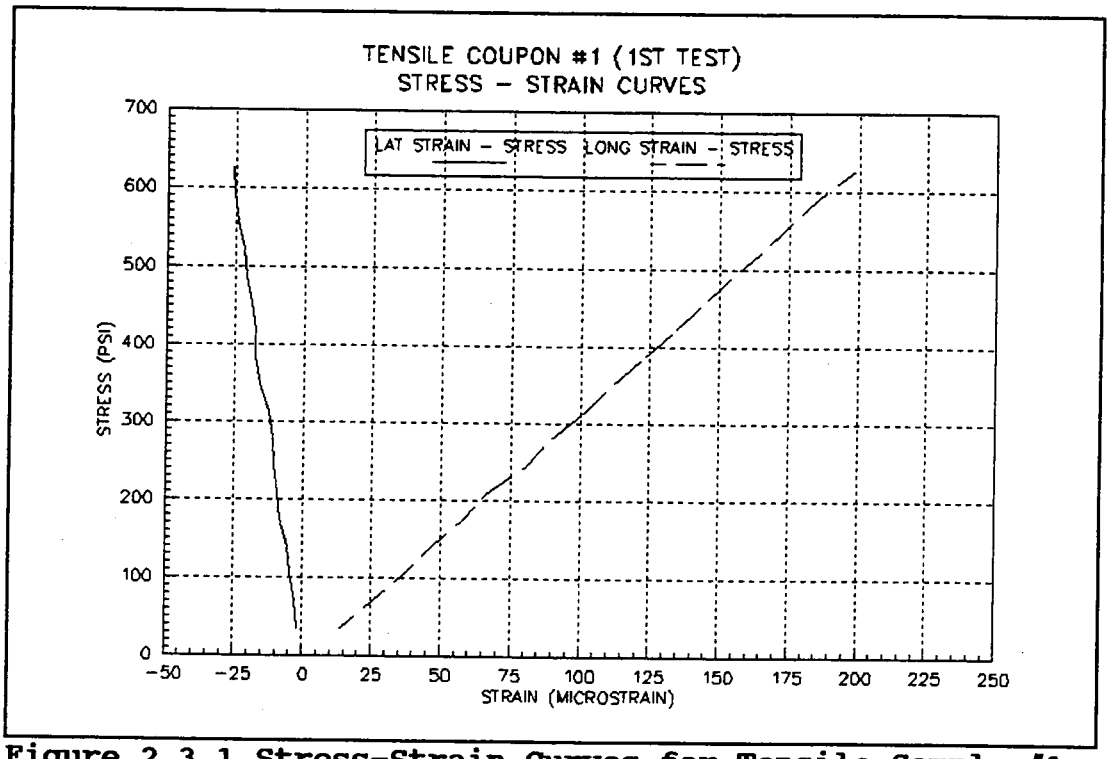


Figure 2.3.1 Stress-Strain Curves for Tensile Sample #1

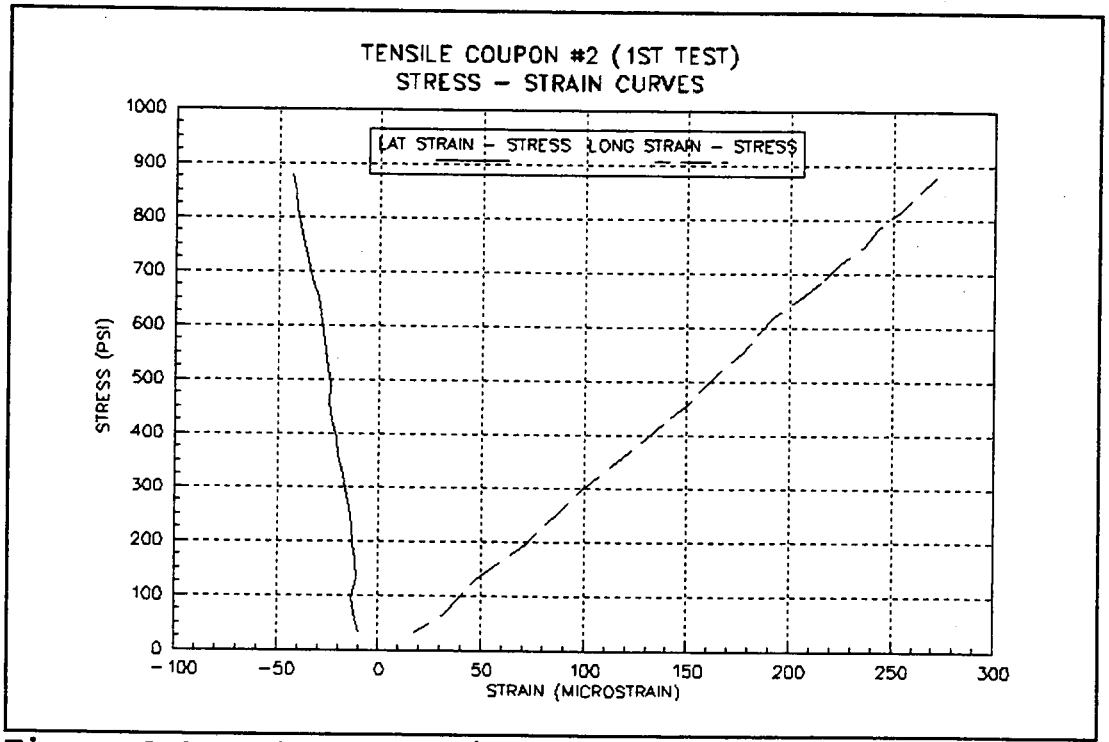


Figure 2.3.2 Stress-Strain Curves for Tensile Sample #2

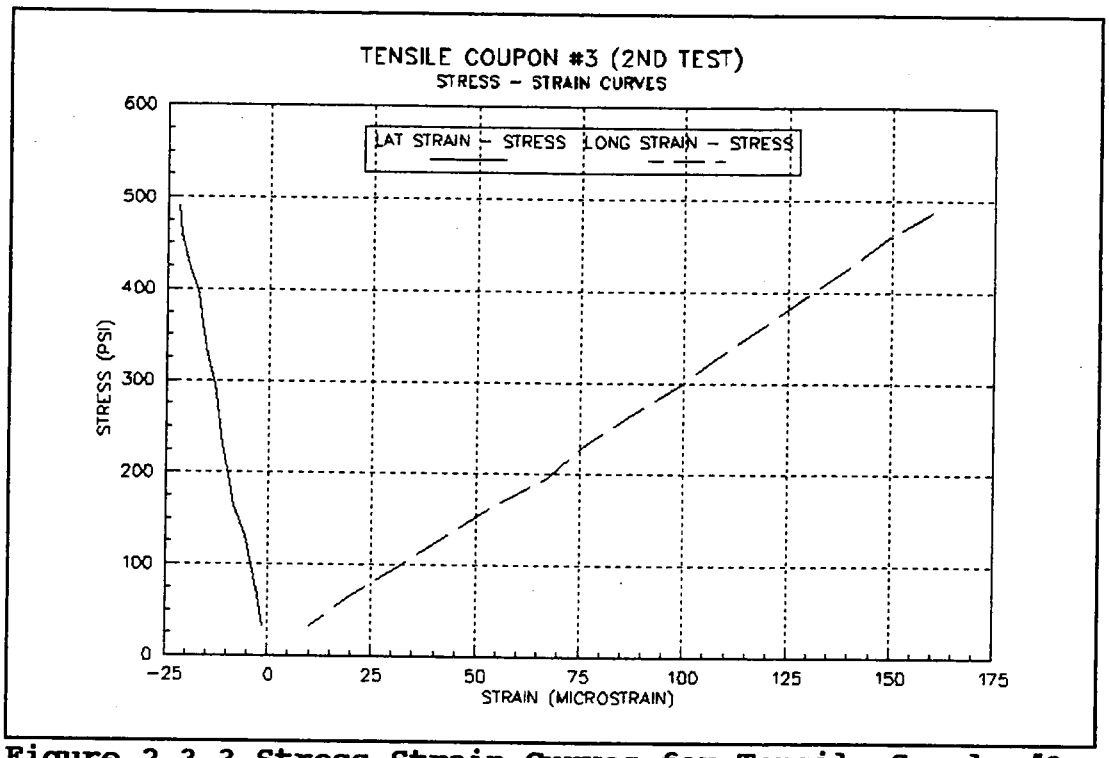


Figure 2.3.3 Stress-Strain Curves for Tensile Sample #3

illustrated are the first test run on the sample. For the third sample, the stress - strain curve is for the second test run on the sample, with the first test possessing a very small ultimate stress of 250 psi. These results lend credence to the theory that either the samples or instrumentation sustained damage in the first tests which rendered the stress - strain curves beyond the first test meaningless.

The material properties calculated for the tensile samples were the same as those calculated for the compressive samples. The modulus of elasticity, E, was calculated using linear regression on 100% of the applied stress. Poisson's ratio was also calculated for the tensile

Tensile Sample #	Test #	Ultimate Tensile Stress, psi	Modulus of Elasticity, psi	Poisson's Ratio
#1	#1	636	3,240,000	0.134
#1	#2	877	2,450,000	0.012
#1	#3	1,010	3,170,000	0.016
#2	#1	894	3,360,000	0.195
#2	#2	205	4,010,000	0.369
#3	#1	189	2,500,000	0.125
#3	#2	515	3,040,000	0.134
Averages		618	3,110,000	0.141
C.O.V.		49.8%	15.9%	79.5%

C.O.V. = Coefficient of Variation

Figure 2.3.4 Tensile Samples Test Results

samples as an average value of Poisson's ratio from zero to the ultimate stress. The results of all these calculations are in figure 2.3.4.

As can be seen by comparing figure 2.3.4 with 2.2.4, the value of Poisson's ratio increased dramatically with tensile testing, for concrete in tension displays fairly brittle behavior (Mehta, 1986).

The values of Poisson's ratio did not vary in the tensile samples as greatly as they did in the compressive samples, as is illustrated in figures 2.3.5 and 2.3.6. Figure 2.3.5 is for the first test run on tensile sample number one, while figure 2.3.6 is for the second test run on this sample. As these figures illustrate, for the tests

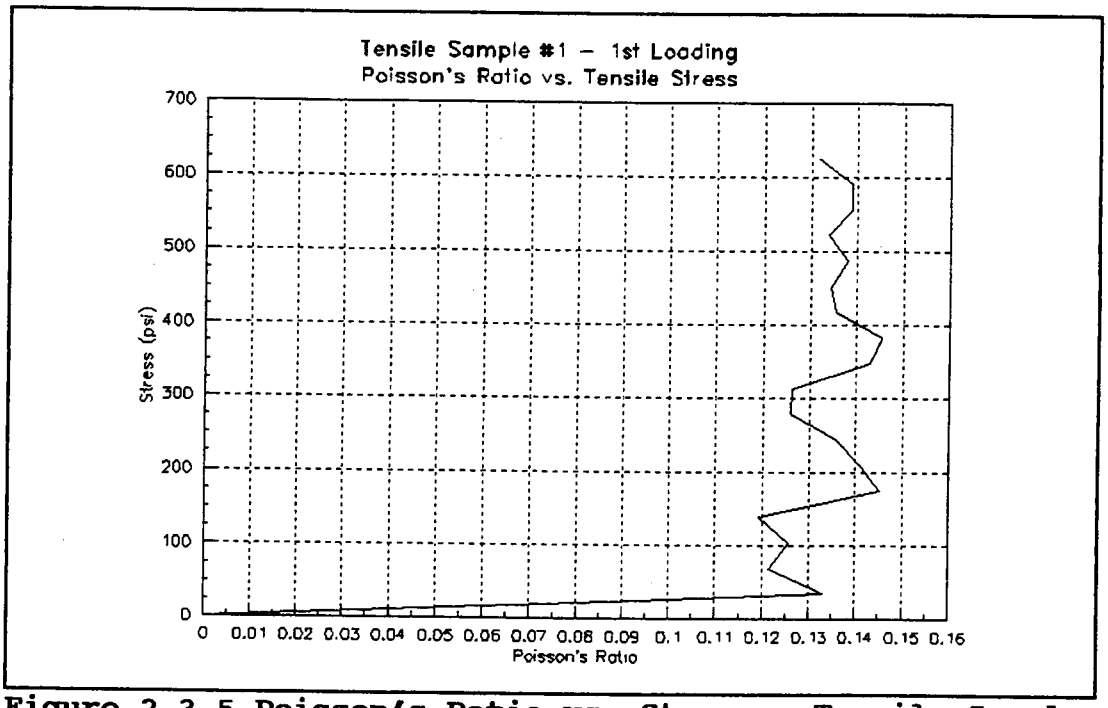


Figure 2.3.5 Poisson's Ratio vs. Stress - Tensile Sample #1 - 1st Test

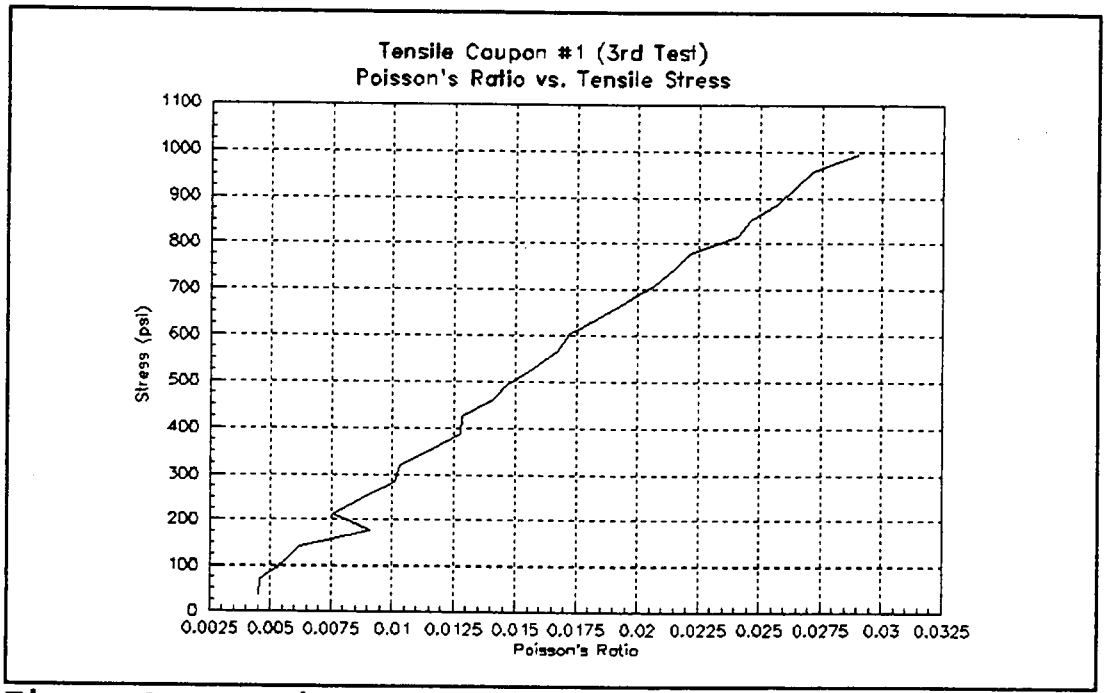


Figure 2.3.6 Poisson's Ratio vs. Stress - Tensile Sample #1 - 2nd Test

with the high tensile stresses, the value of Poisson's ratio remains fairly consistent. Once this high stress level is reached though, Poisson's ratio begins to increase with applied stress. Once again, this is possibly due to one or both of the following factors. First, the slipping and regripping of the sample would cause high local stress concentrations, resulting in possible high strain readings. Also, internal damage caused by earlier testing could cause accelerated lateral expansion as compared to the axial expansion. These and other factors could cause Poisson's ratio to vary.

2.4 Modulus of Rupture Test Results

The data obtained from the modulus of rupture tests were used to calculate the modulus of rupture values for the coupons tested. A total of three modulus of rupture tests were run, with the values obtained from this testing listed in figure 2.4.1.

The modulus of rupture was calculated by using the following formula,

$$M_r = \frac{0.5\ M\ x\ C}{I}$$

Where:

M = ultimate applied moment, pound - inches

Modulus of Rupture Sample #	Ultimate Load pounds	Modulus of Rupture Mr, psi
1	135	1,347
2	180	1,677
3	170	1,596
Averages	162	1,540
C.O.V.	11.9%	9.1%

C.O.V. = Coefficient of Variation

Figure 2.4.1 Modulus of Rupture Samples Test Results

C = 0.5 x depth of sample, inches

I = Moment of Inertia, inches^4

Plummer reported a very large test range of M_r values from 114 psi to 2890 psi (Plummer, 1962). All of the test results obtained fell within this rather broad range. As Plummer stated, there is a direct relation between compressive strength and transverse strength (Plummer, 1962), a fact supported by these test results.

2.5 Absorption Test Results

The reason for measuring the absorption values of the structural clay tile was to find if the tile should be wetted prior to placement. According to the Standard

	1 Hour Boil	5 Hour Boil	Average
Avg 5 Hr. Cold %	11.14	11.03	11.09
Faceshells only	11.10	10.94	11.02
Webs only	11.21	11.23	11.22
Avg 24 Hr. Cold %	11.58	11.49	11.53
Faceshells only	11.53	11.38	11.45
Webs only	11.69	11.71	11.70
Avg 1 Hr. Boil %	11.92		11.92
Faceshells only	11.83		11.83
Webs only	12.09		12.09
Avg 5 Hr. Boil %		12.12	12.12
Faceshells only		11.99	11.99
Webs only		12.37	12.37
Avg. Sat. Coeff.			0.96

Figure 2.5.1 Absorption Samples Test Results

Building Code (SBCC, 1992), structural clay tile having absorptions (1 hour boil) of 12% or more shall be wetted prior to placing. The results from the absorption tests are listed in figure 2.5.1. As stated earlier in section 2.1, a total of fifteen absorption samples were tested. Of these fifteen, ten were faceshell pieces and the remaining five were web pieces. This sampling was done in accordance with ASTM C67 7.2.2 (ASTM, 1991), which was the specification used to run this test.

The formulas used to calculate the values of the absorption were as follows. The formula for both 5 hour and

24 hour cold water absorption was,

$$Absorption, \% = 100 \frac{W_s - W_d}{W_d}$$

Where:

W_s = saturated weight of sample after cold water submersion, grams

W_d = dry weight of sample, grams

The values for both the 5 hour and 24 hour cold water absorption percentage are given in figure 2.5.1.

The formula used to calculate the 1 hour and 5 hour boiling water absorption was,

$$Absorption, \% = 100 \frac{W_b - W_d}{W_d}$$

Where:

W_b = saturated weight of sample after boiling water submersion, grams

W_d = dry weight of sample, grams

The values for both the 1 hour and 5 hour boiling water absorption percentage are given in figure 2.5.1, as well as the averages of both the 1 hour and 5 hour boil tests.

The formula used to calculate the saturation coefficient was,

$$Saturation\ Coefficient = \frac{W_{s_2} - W_d}{W_{b_5} - W_d}$$

Where:

W_{s2} = saturated weight of the specimen after 24 hour submersion in cold water, grams

W_{b5} = saturated weight of the specimen after 5 hour submersion in boiling water, grams

W_d = dry weight of the specimen, grams

The 1992/93 revisions of the Standard Building Code specifies in section 1409.8.2 that structural clay tile having absorptions (1 hour boil) of 12% or more shall be wetted before laying (SBCC, 1992). The results from the absorption tests came out to be 11.92%. Although the strict letter of the code would be met by not wetting this tile, it may be possible that by not wetting this tile that the bond strength could be lowered.

Another pattern which developed during this testing was the difference in the absorption rate between the faceshell pieces and the web pieces. This difference is only slight, with a maximum difference of 0.38% in the 5 hour boil rate, but is noticeable. One possible explanation for this difference is in the tile manufacturing process. The tile is extruded through a mold, and then fired for a certain period of time. Following this firing period, the tile is allowed to cool back down by lowering the temperature in the kiln slowly. When this temperature is lowered, the outside

of the tile cools quicker than the interior of the tile, thus driving more moisture from the cells in the interior, or web, pieces. This difference in the cooling rate may account for the difference in the absorption rates between the two sections, as the web pieces would have less initial moisture present.

The saturation coefficient is a measure of how much additional cell space is filled with water when the sample is subjected to boiling. For the tests run, the average value of this saturation coefficient came out to 0.96. This means that 96% of the cell space occupied by water was occupied previous to the boil test. Plummer gave ranges of the saturation coefficient from 0.16 to 1.00, with the majority falling between 0.66 to 0.90 (Plummer, 1962). The values calculated above are slightly higher than these, but Plummer's tests were run on brick, not structural tile. Although a direct comparison cannot be made, the tests run fell into Plummer's range. The maximum allowable saturation given by ASTM C34 - 84, for grade LBX tile, is 16% maximum water absorption by 1 hour boiling test (ASTM, 1984). This corresponds to a saturation coefficient of 0.84. This allowable value is based on a sampling of five tile with no one tile allowed to exceed 19% absorption in an one hour boil test. All of the saturation coefficients calculated for the absorption tests came well within these bounds.

Chapter 3

TESTING PROCEDURES AND RESULTS OF MORTAR CYLINDERS

Introduction

The following chapter discusses the mortar cylinder testing which was performed. These mortar cylinders were 2 inches in diameter and 4 inches in height. The reasons for performing these tests were both to obtain the material properties of these samples under compressive loading, and also to gain an insight into how the mortar interacts with the structural clay tile. A total of twelve mortar cylinders were tested in compression and six in split cylinder tension. Air dried versus moist cured mortar cube strengths are also compared.

3.1 Mortar Cylinder Preparation and Testing

The cylinders were prepared in a standard brass mold according to ASTM preparation specifications. The mortar was 1 part type N masonry cement, mixed with 2 1/2 parts natural river sand and water. The samples were prepared, allowed to dry for 24 hours, and moved to a moisture room until testing. Following approximately 28 days in the moisture room, the cylinders were removed and allowed to dry for approximately 48 hours. After drying, three cylinders were marked and had MBond 200 epoxy applied on both sides of

the cylinder. After allowing the epoxy to dry for a period of 48 hours, strain gages were applied to the cylinders, with MBond 200 epoxy. These strain gages were designed such that two gage patterns were present on one gage, allowing both lateral and longitudinal strains to be read.

Following the attachment of the strain gages, the cylinders were taken into the testing room and the strain gages were wired into a STB 884/SCV terminal block. This terminal block was connected, via a 32 pin data cable, to the data collection system. The data collection system consisted of an IBM PS/2 mated via an IEEE 488 interface with a Megadac 3008 data collection system. Both load and strain readings were recorded on this system. The sampling rate was kept at 10 samples per second.

The machine used to test the cylinders was a Tinius-Olsen Universal Testing machine with a 120,000 lb. capacity. This machine has three load ranges with the middle load range chosen for the cylinder testing. This chosen range was 0 to 60,000 lbs. with 100 lb. graduations. This range was chosen because of the smaller load graduations.

The cylinders were placed into the machine and loaded in compression until failure. The loading rate was kept under 2000 lbs/minute, with load levels recorded on the data collection system every 500 pounds. The data collection system also recorded 4 strain readings. These readings were front lateral strain, back lateral strain, front

longitudinal strain, and back longitudinal strain. The load levels were recorded by use of a "doorbell" device, which simply input an electrical surge into the data collection system.

The samples were loaded in two different fashions. The first two samples were loaded up to ultimate and then the load was lowered with load readings and strain readings being taken on the unloading side. This was done in an effort to obtain some post-peak stress-strain data. However, once the ultimate load was reached the cylinder may have cracked resulting in damage to the strain gages. The third cylinder was loaded in three cycles. The first cycle was from 0 to 5,000 lbs, the second cycle was from 0 to 9,000 lbs, and the third and final cycle was from 0 to failure, which came out to be 11,000 lbs. The cyclic loading was performed in an effort to obtain data on the load - unload behavior of the mortar. The cycles were based on the ultimate loads of the first two cylinders.

3.2 Mortar Cylinder Test Results Under Monotonic Loading

The first two mortar cylinders tested were loaded in a monotonic fashion in which the load was simply increased from zero to ultimate. These data were used to obtain both stress - strain curves for the samples as well as to determine some material properties for the samples.

The data were first used to obtain stress - strain curves for the samples. These curves are shown in figures 3.2.1, 3.2.2, and 3.2.3. The first two figures reflect data obtained from the first mortar cylinder test. The difference in the two is that the first graph (figure 3.2.1) has post ultimate stress data while the second graph (figure 3.2.2) has data up to ultimate stress only. It is arguable that the post ultimate stress data should be excluded because of the possible damage the cylinder received in loading up to ultimate. The pattern which the graph reflects in the post ultimate stress data is possibly inaccurate because of this possible damage. In any case, the data collected up to ultimate stress should be considered the only reliable data. As can be seen in figures 3.2.1, 3.2.2, and 3.2.3 the lateral stress - strain curve remains fairly linear up to approximately 60 to 70% of the ultimate stress. While the longitudinal stress - strain curves also reflect this linear behavior, these curves also show a faster increase in longitudinal strain than in lateral strain.

The table in figure 3.2.4 gives the material properties obtained from the mortar cylinder tests. The modulus of elasticity, E, was calculated using linear regression on the stress - strain curves. This regression was performed on the data from 0 stress up to 50% of the ultimate stress. The percentage difference between the lowest E and highest E

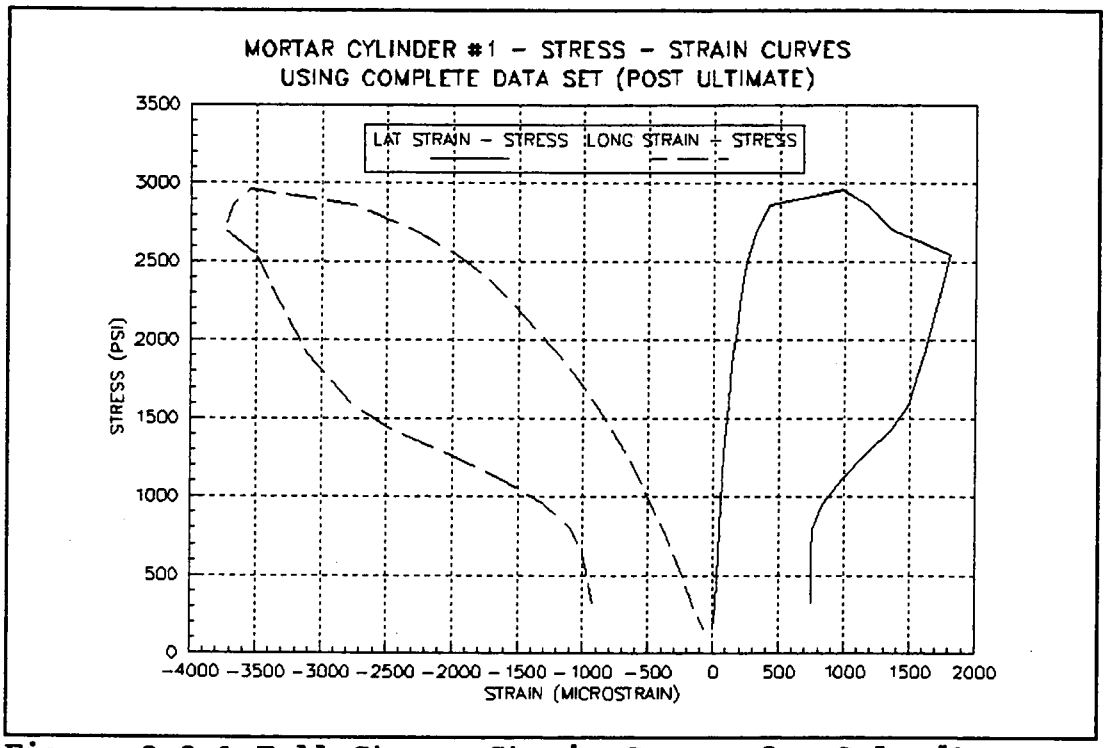


Figure 3.2.1 Full Stress-Strain Curves for Cyl. #1

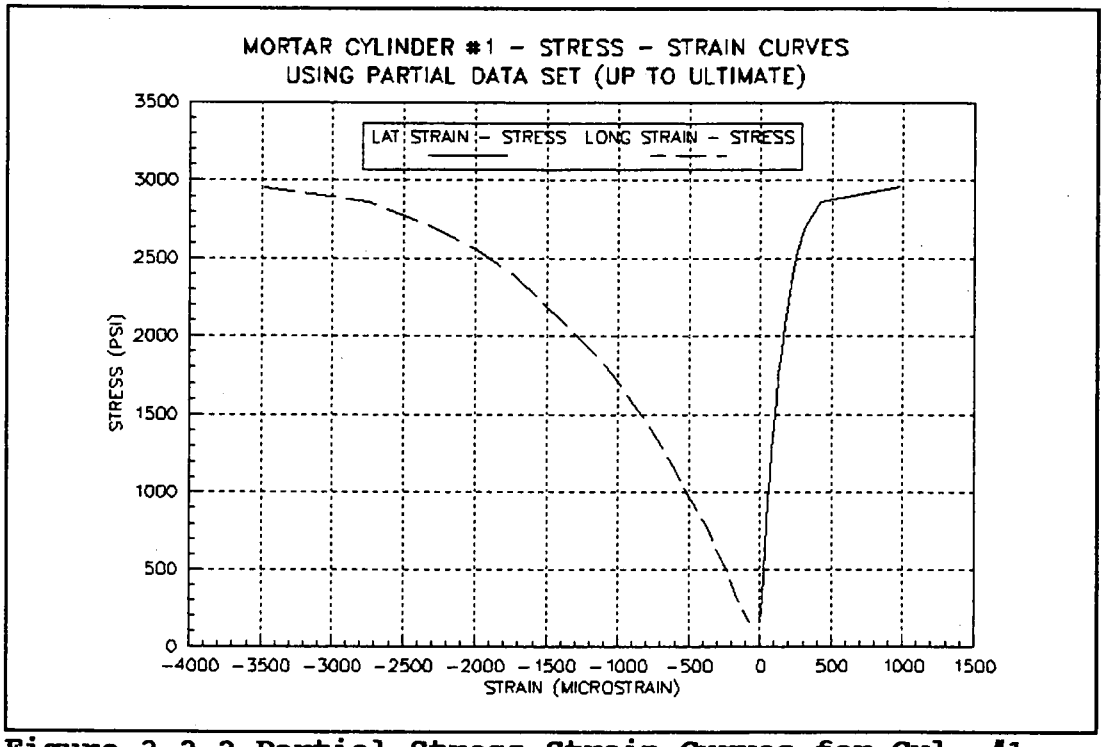


Figure 3.2.2 Partial Stress-Strain Curves for Cyl. #1

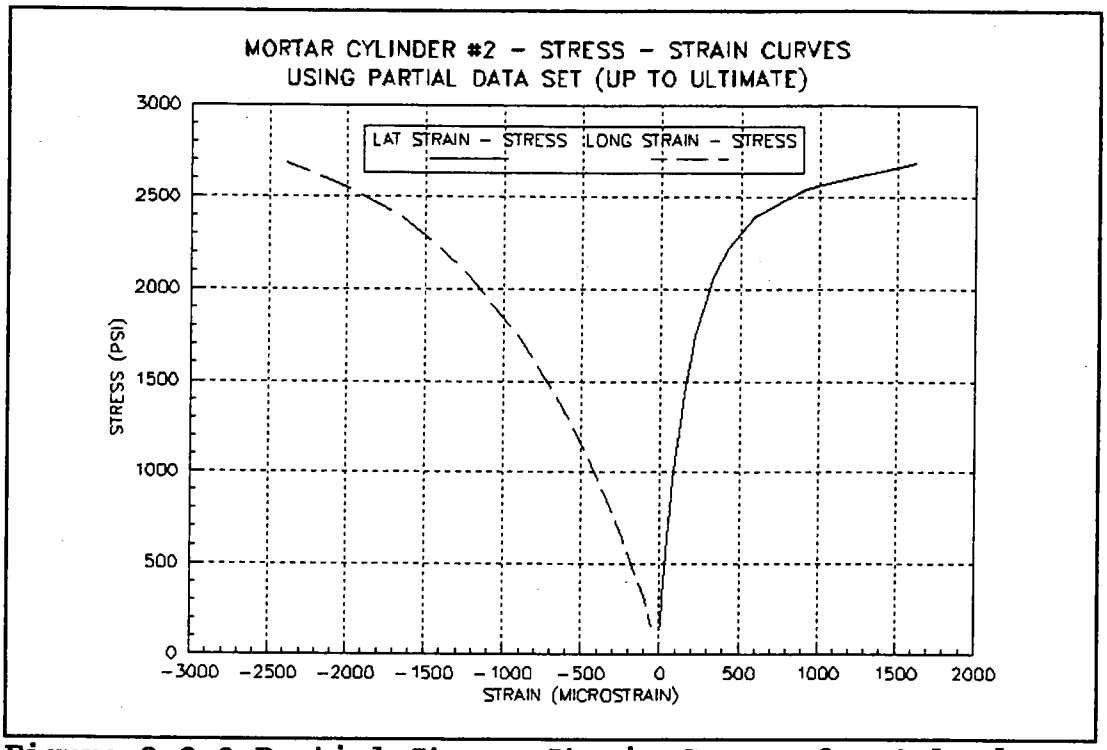


Figure 3.2.3 Partial Stress-Strain Curves for Cyl. #2

Mortar Cylinder Sample #	Ultimate Stress, psi	Modulus of Elasticity, psi	Poisson's Ratio
1	2,960	1,800,000	0.122
2	2,690	2,140,000	0.217
3	3,500	2,070,000	0.126
Averages	3,050	2,000,000	0.155
C.O.V.	11.0%	7.3%	28.3%

C.O.V. = Coefficient of Variation

Figure 3.2.4 Mortar Cylinder Samples Test Results

was only 15%, which is small in a limited sampling such as this. The average value for E obtained in these tests, approximately 2,000,000 psi, seems reasonable. The value of E for concrete in compression given by Mehta (1986) ranges from 3,100,000 to 5,700,000 psi. The values obtained in these tests are reasonable when compared to these values of E for concrete.

The other material property values given in figure 3.2.4 are for Poisson's ratio. Poisson's ratio, ν, is calculated as follows,

$$\nu = -\frac{lateral\ \epsilon}{axial\ \epsilon}$$

Figures 3.2.5 and 3.2.6 show Poisson's ratio plotted against the applied compressive stress. These figures show how Poisson's ratio increases with applied stress and also demonstrate how the cylinders possibly expand laterally more quickly than it is shortening.

The values set forth in figure 3.2.4 for Poisson's ratio are the values of Poisson's at 50% of the ultimate stress. Poisson set the value at approximately 0.25 for isotropic materials (Gere and Timoshenko, 1990). Poisson's ratio for concrete, which is given as approximately 0.10 to 0.20 (Mehta, 1986), is in approximate agreement with these results.

Figure 3.2.7 lists the ultimate loads and compressive

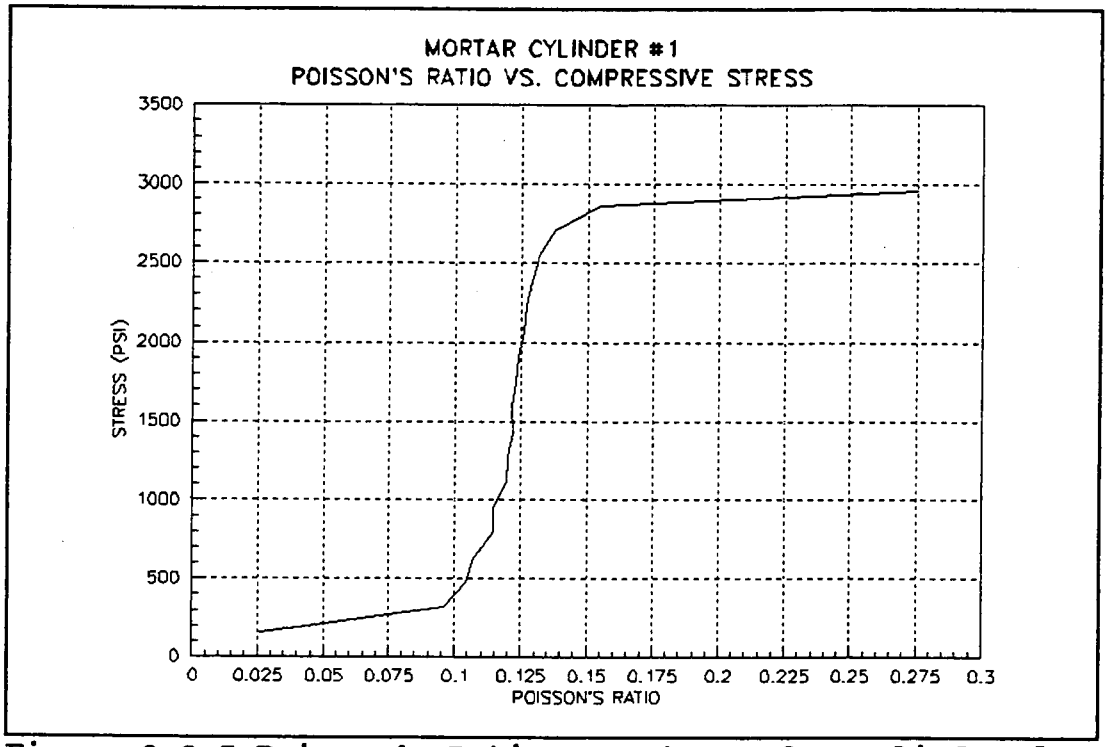


Figure 3.2.5 Poisson's Ratio vs. Stress for Cylinder #1

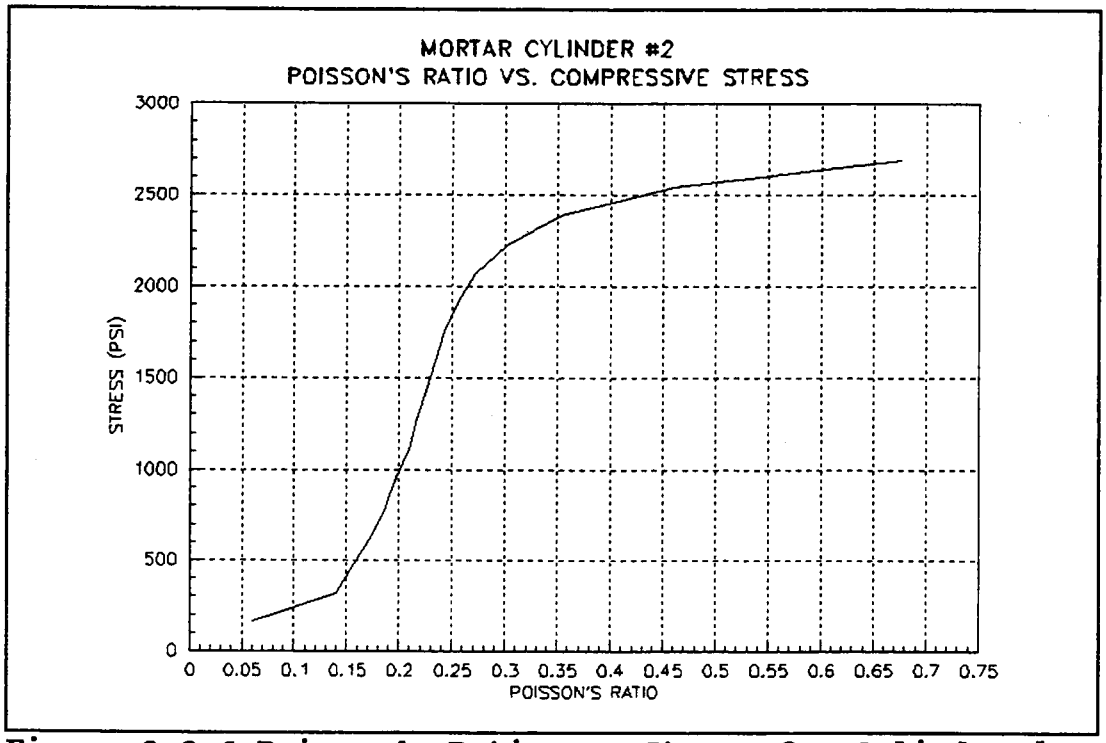


Figure 3.2.6 Poisson's Ratio vs. Stress for Cylinder #2

	Mortar Batch #1		Mortar Batch #2		Mortar Batch #3	
Cylinder #	Ultimate Load, lbs	Ultimate Stress, psi	Ultimate Load, lbs	Ultimate Stress, psi	Ultimate Load, lbs	Ultimate Stress, psi
1	9,250	2,940	8,400	2,670	11,800	3,760
2	8,950	2,850	8,600	2,740	11,600	3,690
3	10,350	3,290	8,800	2,800	10,600	3,370
4	9,300	2,960	8,450	2,690	11,000	3,500
Average	9,460	3,010	8,560	2,730	11,250	3,580
C.O.V.	5.6%	5.5%	1.8%	1.8%	4.2%	4.3%

Average Ultimate Stress = 3100 psi
Average Stress C.O.V. = 12.2%
C.O.V. = Coefficient of Variation

Figure 3.2.7 Mortar Cylinders Applied Loads and Stresses

stresses of all twelve cylinder samples, along with batch and overall averages. All cylinders exceeded the minimum required compressive strength of type N mortar of 750 psi.

3.3 Mortar Cylinder Test Results for Cyclic Loading

This section is concerned with the cyclic loading which was done on cylinder #3. While the material properties of E and ν were calculated and presented in section 3.2, this section discusses the stress - strain behavior of the cylinder under cyclic loading.

There were three loading cycles performed on cylinder #3. The first cycle went from 0 lbs to 5000 lbs to 0 lbs, the second cycle from 0 lbs to 9000 lbs to 500 lbs, with the

third cycle from 500 lbs to 11,000 lbs, with 11,000 lbs being the ultimate load applied. The cycles were based on the breaking strengths of the two previous samples, with the thought being that only two cycles would be done. However, when testing the cylinder, the load held at 9000 lbs, and the decision was made to cycle the load down to 500 lbs and back to ultimate. The reason for cyclic loading was to see if the cylinders displayed elastic behavior when loaded below their ultimate strengths.

The stress - strain graphs obtained from the cyclic loadings are presented in figures 3.3.1, 3.3.2, 3.3.3, 3.3.4, and 3.3.5. Figure 3.3.1 represents the first loading cycle performed, with figure 3.3.2 representing the second loading cycle, and figure 33.3 represents the third loading cycle. Figures 3.3.4 and 3.3.5 display all three loading cycles with figure 3.3.4 showing lateral strains versus applied stresses and figure 3.3.5 showing longitudinal strains versus applied stresses.

As can be seen in figures 3.3.1 and 3.3.2, the mortar cylinders display fairly linear-elastic behavior. The first two load cycles exhibit a linear stress - strain relationship on both the loading and unloading portions of the graphs. The unloading portion is almost parallel to the loading portion, and an initial offset is visible in both the lateral and longitudinal graphs. This linear behavior is also visible in the third cycle loading (figure 3.3.3),

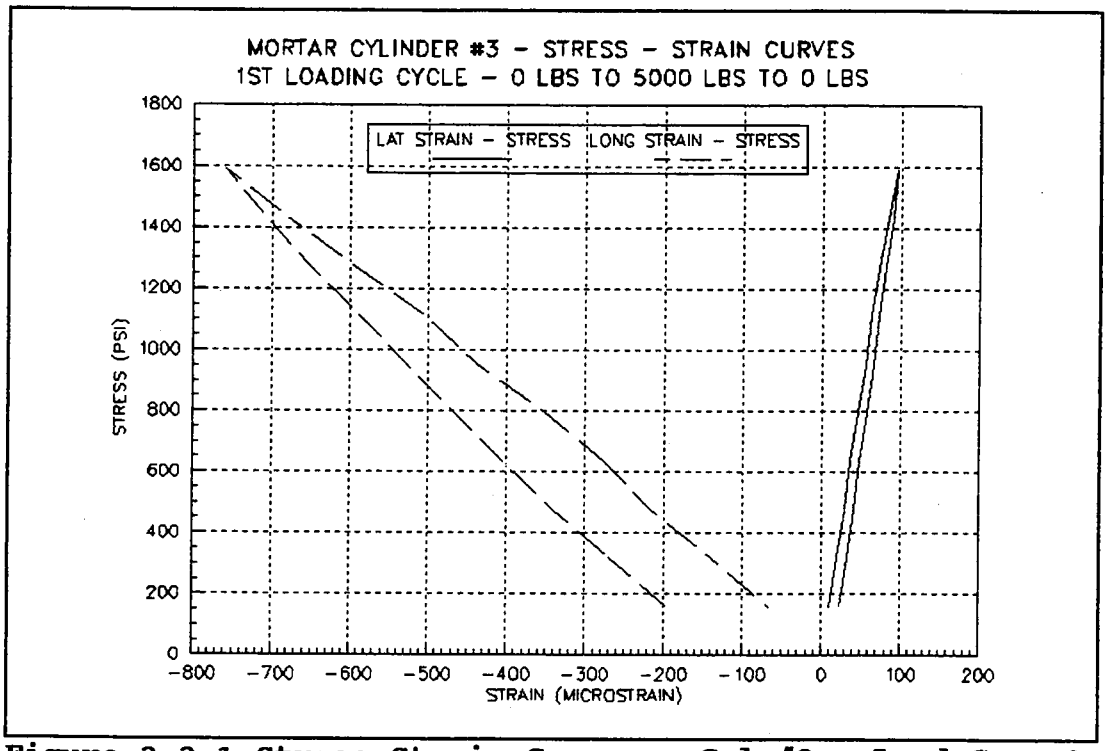


Figure 3.3.1 Stress-Strain Curves - Cyl.#3 - Load Cyc. 1

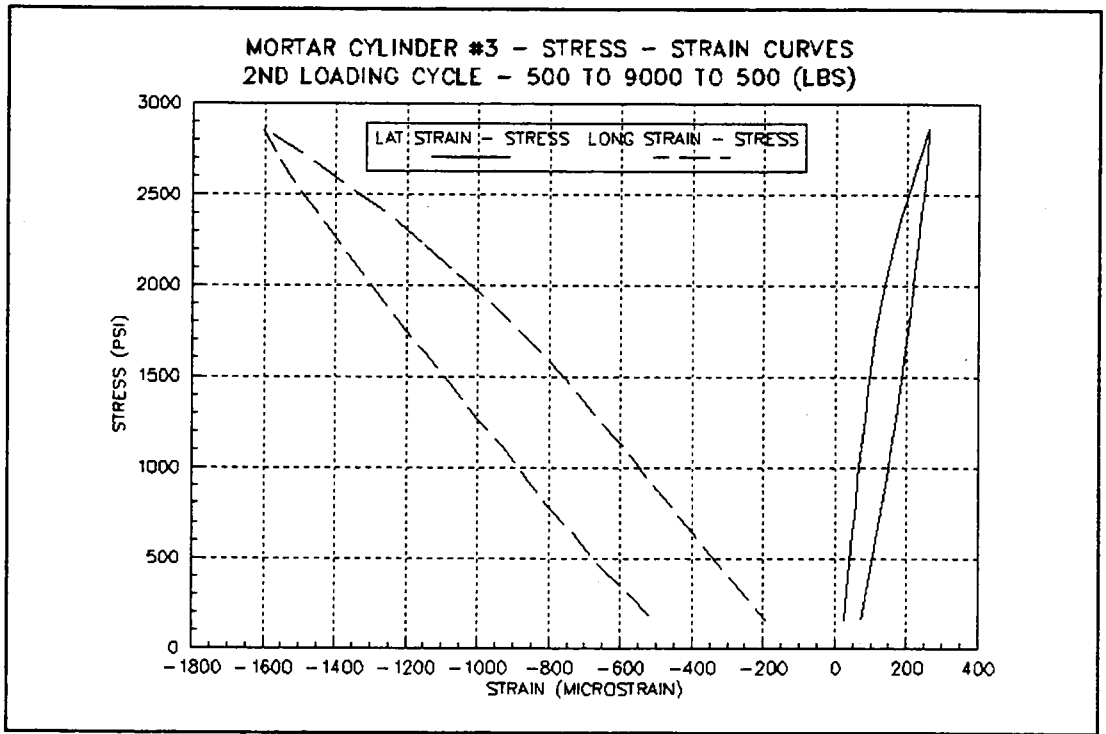


Figure 3.3.2 Stress-Strain Curves - Cyl.#3 - Load Cyc. 2

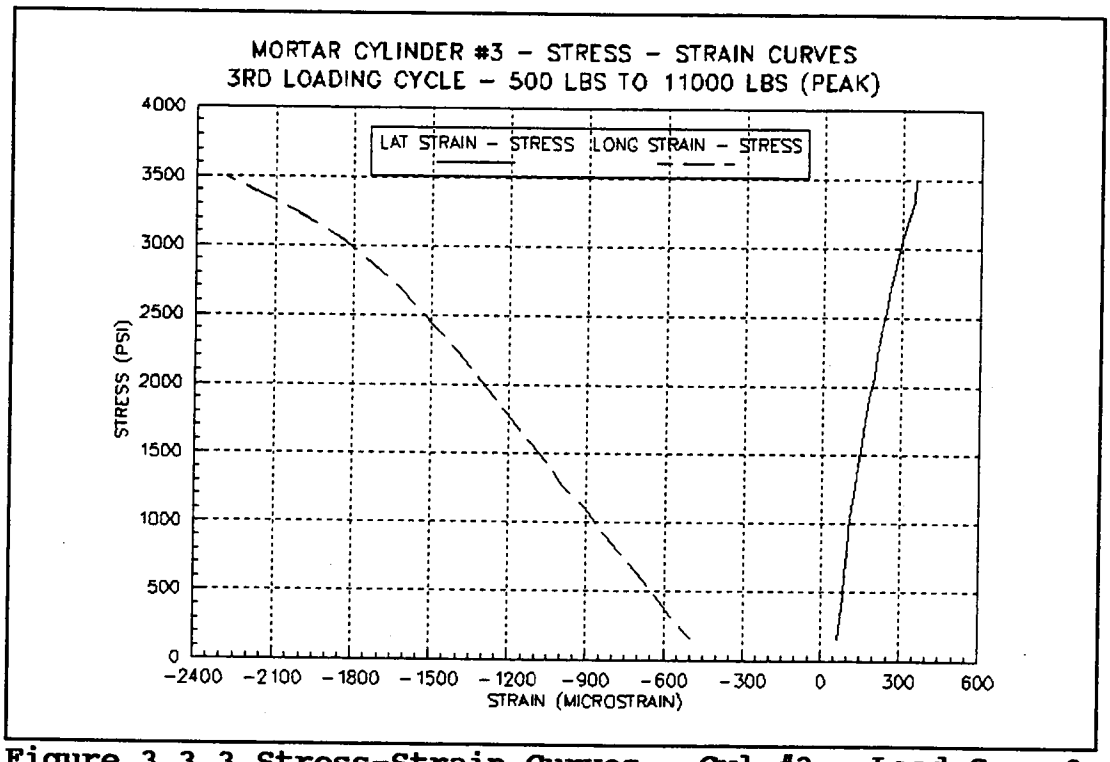


Figure 3.3.3 Stress-Strain Curves - Cyl.#3 - Load Cyc. 3

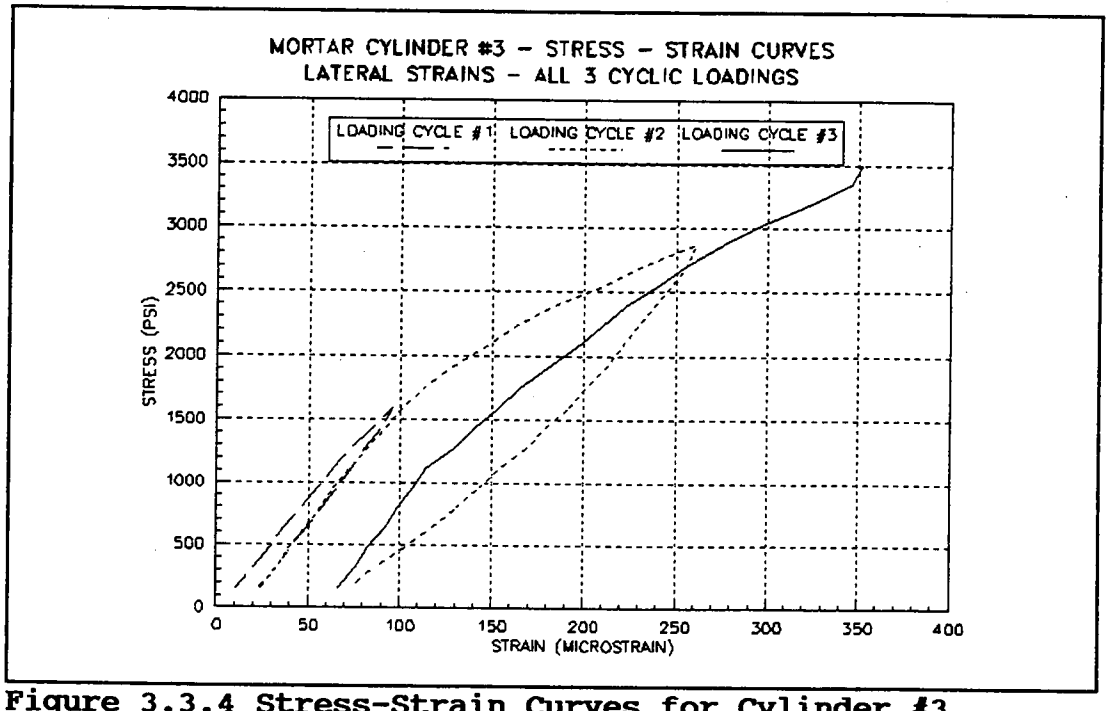


Figure 3.3.4 Stress-Strain Curves for Cylinder #3 Stress vs. Lateral Strains for all Load Cycles

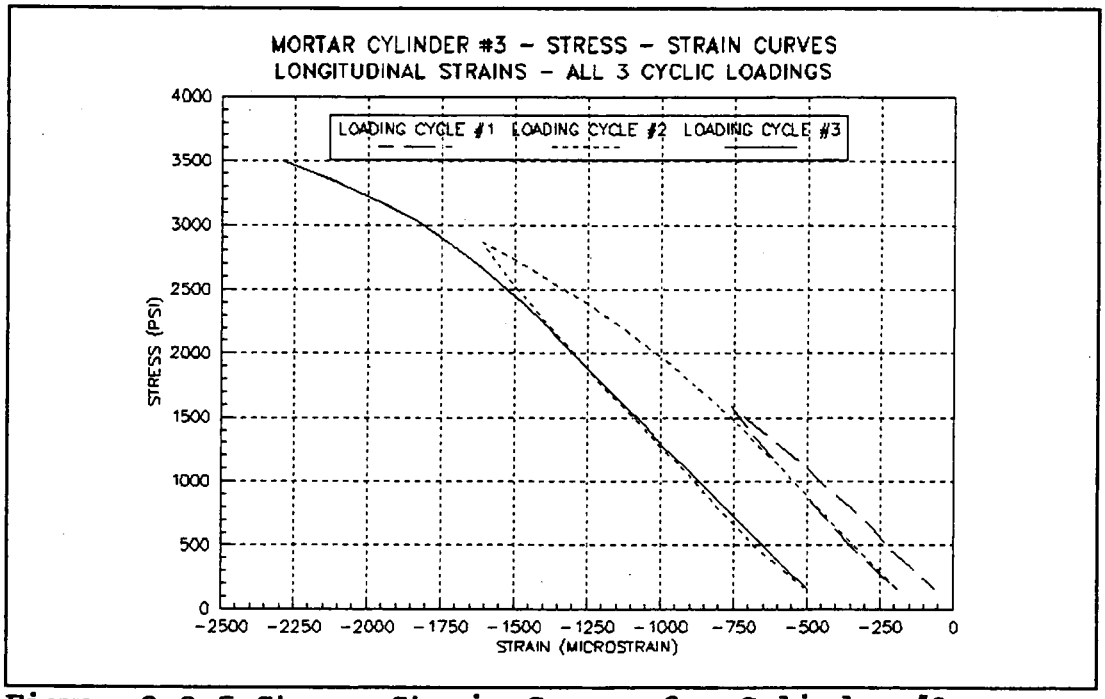


Figure 3.3.5 Stress-Strain Curves for Cylinder #3 Stress vs. Longitudinal Strains for all Load Cycles

up to approximately 70% of the ultimate stress, consistent with the non-cyclic loaded cylinders. These cylinders were also fairly linear up to approximately 70% of their ultimate stress.

The graphs shown in figures 3.3.4 and 3.3.5 show that this linear behavior also carries over to different loading cycles. The unload portions of cycles #1 and #2 are closely followed by the loading portions of cycles #2 and #3, respectively. This behavior is observed in both the lateral and longitudinal cases, although it is more evident in the longitudinal case.

The reload portions of the stress - longitudinal strains are fairly linear for approximately 40 to 50% of the

Load Cycle	E, psi	% Diff.
1st	2,070,000	0.0
2nd (1st reload)	2,400,000	15.9
3rd (2nd reload)	2,290,000	10.6
Avg. Reload	2,345,000	13.3

Figure 3.3.6 Reload Modulus Calculation Results

reload cycle. Values of a reload modulus are shown in figure 3.3.6. The modulus values for the reload portions did not vary by over 15.9% from the original value of E calculated in the first load cycle.

3.4 Test Results for Split Tensile Samples

A total of six cylinders were made from each mortar batch. Of these six, four were tested as compressive samples and the other two were tested as split tensile samples. These split tensile tests were conducted in accordance with ASTM C780, and the tests were performed on the Tinius-Olsen Universal Testing Machine mentioned earlier in this chapter. The samples were tested by laying

	Mortar Batch #1		Mortar Batch #2		Mortar Batch #3	
Split Cylinder #	Ultimate Load, lbs	Split Tensile Stress, psi	Ultimate Load, lbs	Split Tensile Stress, psi	Ultimate Load, lbs	Split Tensile Stress, psi
1	3,360	268	3,090	246	4,270	340
2	3,430	273	3,030	241	3,680	293
Averages	3,395	271	3,060	244	3,975	317
C.O.V.	1.0%	0.9%	1.0%	1.0%	7.4%	7.4%

Average Split Tensile Stress = 277 psi
Average Split Tensile C.O.V. = 12.0%
C.O.V. = Coefficient of Variation

Figure 3.4.1 Split Tensile Test Results

the cylinders horizontally on the loading table and loading along the diameter until the samples split.

The results from these tests are shown in figure 3.4.1, which lists the ultimate applied loads as well as the ultimate split tensile stresses. These stresses were calculated by the following formula,

$$T = \frac{2P}{\pi l d}$$

Where:

T = Split tensile strength, psi

l = length of cylinder, in.

d = diameter of cylinder, in.

The split tensile test is an approximate measure of the tensile strength of a material. Another method of approximating the tensile strength of a material is to calculate the modulus of rupture f_r. According to Park and Paulay (Park and Paulay, 1975), the split tensile strength usually ranges from 50 to 75% of the modulus of rupture. The modulus of rupture is approximated by the following formula,

$$f_r = K\sqrt{f'_c}$$

where K varies from 7 to 13 for concrete (Park and Paulay, 1975). Estimating that the average split tensile strength which was obtained was 50% of the modulus of rupture results in a K value of approximately 10 for the mortar cylinders. This falls within the range of K values given for concrete.

3.5 Air Cure vs. Moist Cure Test Results

The mortar cylinders used in these tests were moist cured for a period of approximately 25 days and then were allowed to dry for 3 days, so the epoxy and strain gages could be applied. Miltenberger et al. (1993) explored the relationship between moist cured and dry cured mortar samples. They concluded that air dried mortar samples display a higher compressive strength than moist cured mortar samples. In an effort to verify the findings of this article, two sets of mortar cube samples were made from the

Sample #	Moist Cured Ultimate Stress, psi	Air Cured Ultimate Stress, psi	% Increase
1	1,513	2,100	
2	1,588	2,062	
3		2,138	
Averages	1,551	2,100	35.4
C.O.V.	2.4%	0.9%	

C.O.V. = Coefficient of Variation

Figure 3.5.1 Air Cured vs. Moist Cured Comparisons

same mortar batch, with one set air cured and the other set moist cured. Both samples were allowed to cure for 25 days and then broken. As shown by figure 3.5.1, the air cured samples displayed higher compressive strengths than the moist cured.

The possible reasons for the higher compressive strengths displayed by the air cured samples included carbonation, crystallization, and increased pore pressure in moist cured samples (Miltenberger et al., 1993). Carbonation limits the rate of carbon dioxide diffusion while crystallization causes additional depositing of calcium hydroxide. Both of these occur when the sample is losing moisture and both add to the compressive strength of

the mortar. The increased pore pressure occurs when the sample is being tested. As the sample is compressed, the moist cured samples may exhibit increases in pore pressure thus leading to premature failures and ultimate strengths.

As shown by figure 3.5.1, the dry cured samples displayed an average increase of 35.4% in ultimate strength. This increase is higher than the increase found by Miltenberger et al. (1993), which averaged around 12%. The increase in the ultimate strength reinforces the findings of Miltenberger et al. (1993), and also demonstrate how sample curing methods can affect mortar strength.

Chapter 4

TESTING PROCEDURES AND RESULTS OF MINIATURE PRISMS

Introduction

This chapter covers the miniature prism testing which was performed. These miniature prisms were simply two 8-inch structural clay tiles laid up using a stack bond with a 3/4 inch mortar joint. Four miniature prisms were tested, all in compression loading. These prisms were tested to both gain data on their behavior, and to also compare the results with larger prism tests.

4.1 Miniature Prism Preparation and Testing Procedures

The prisms were prepared by laying up two structural clay tile using 1 part type N masonry cement, mixed with 2 1/2 parts natural river sand and water. The mortar joint was a full bed joint and was approximately 3/4 inch thick.

After allowing approximately 24 hours for the mortar to dry, the prisms were strapped together, using 1/2 inch metal strapping material. This was done so the prisms could be moved to the testing machine.

After the prisms were strapped and moved, they were capped with hydrocal cement. Because of the importance of obtaining parallel capping surfaces, the prisms were capped in the same manner as previous unit tile tests (Flanagan et al., 1993). A 3 foot by 2 foot by 1 inch thick metal plate

with leveling screws, was used to cap the specimens. The plate was first leveled and then oiled. The hydrocal cement was prepared by mixing with water and then poured onto the plate. The prism was then lowered by hand into the hydrocal and the prism was leveled. After allowing the hydrocal to dry, the prism was removed, and the capping procedure was repeated for the other end of the prism.

After capping the prisms and allowing them to age for fourteen days, the prisms were instrumented and tested. The instrumentation used on the prisms were 1 inch linear variable displacement transducers (LVDTs). A total of 4 LVDTs were used, with one LVDT placed on each corner of the prism. Mounting was accomplished by placing the LVDTs in a mounting bracket and using 2" by 2" angle iron as stops. The brackets and stops were attached to the prisms using a hot glue gun. The LVDTs were mounted such that the gage length was evenly divided on both sides of the mortar joint. The gage length was 7 1/2" for all LVDTs. Also used in the instrumentation was a "doorbell". The "doorbell", as described in earlier chapters, was used to record load levels every 1000 pounds.

The instrumentation was wired into a STB 884/SCV terminal block. This block was attached, via 32 pin data cable, to the same Megadac 3008 data collection system used in the other tests. The sampling rate was kept at 3 samples per second.

The machine used to test the prisms was the Tinius-Olsen Universal Testing machine used in the other tests. Because of the assumption that the prisms would fail at approximately 50 kips, the highest range of the machine was used.

The prisms were capped, placed in the testing machine, instrumented, photographed, and then loaded in cyclic fashion until failure. The loading rate was approximately 5,000 lbs/minute, with load spikes recorded every 1,000 lbs. The first and fourth prisms were loaded from 0 to 20,000 lbs. and then unloaded. The LVDTs were then removed, and the prisms were reloaded until failure. The second and third prisms were loaded to 30,000 lbs before unloading and removing the LVDTs. As before, these prisms were then reloaded until failure. The reason for the difference in the loading patterns was in the prism behavior. The first and fourth prisms exhibited cracking earlier than the other prisms, and were thus taken to a smaller load before the LVDTs were removed. After failure, photographs were taken, and then the machine was cleaned for the next test.

4.2 Prism Strength Test Results

The prisms were tested, and then the data was used to both plot stress - strain curves, as well as to calculate the modulus of elasticity, E. The stress - strain curves, shown in figures 4.2.1, 4.2.2, 4.2.3, and 4.2.4, plot the

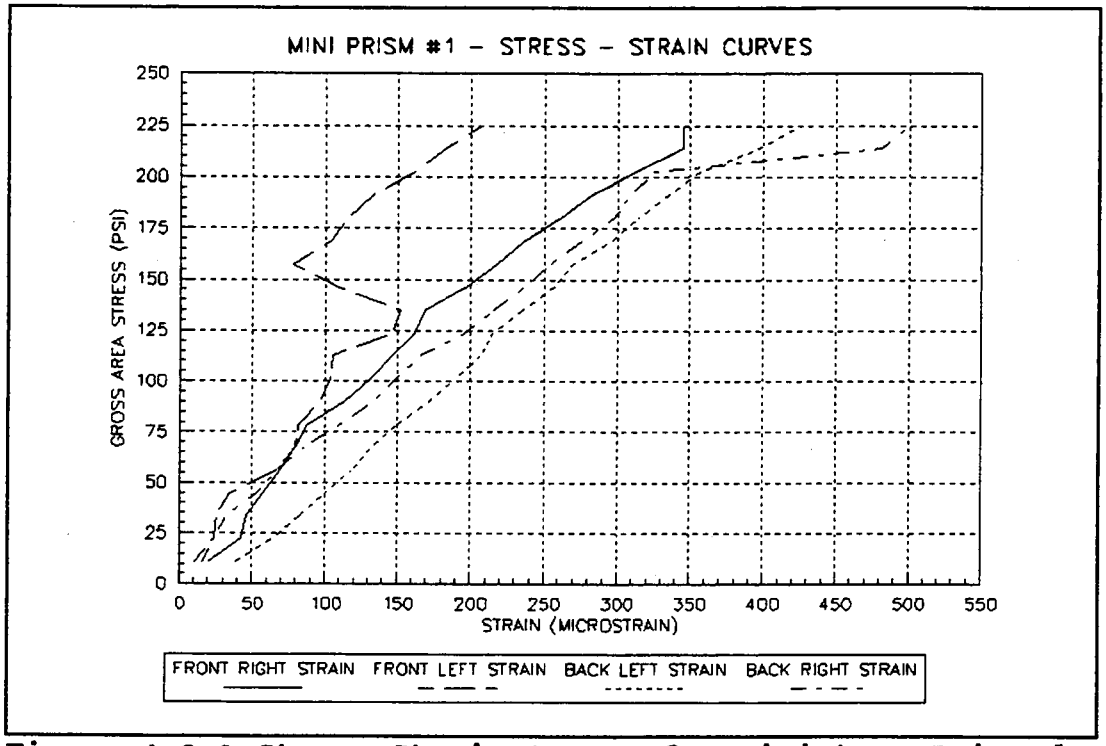


Figure 4.2.1 Stress-Strain Curves for Miniature Prism #1

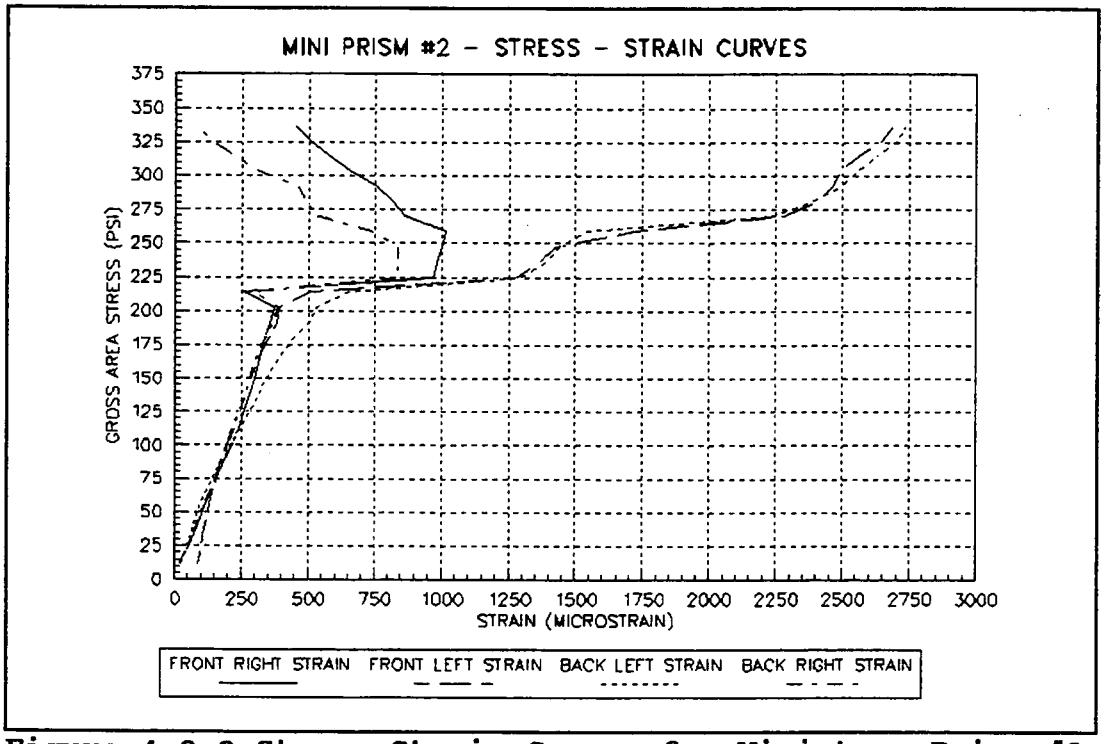


Figure 4.2.2 Stress-Strain Curves for Miniature Prism #2

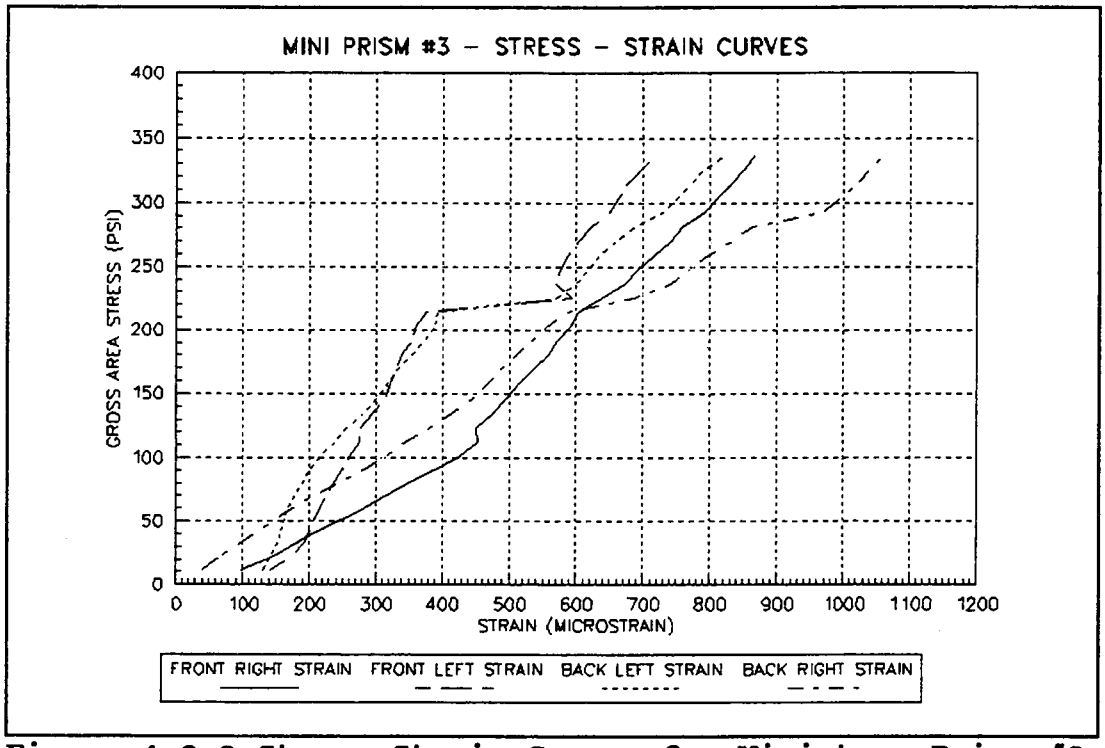


Figure 4.2.3 Stress-Strain Curves for Miniature Prism #3

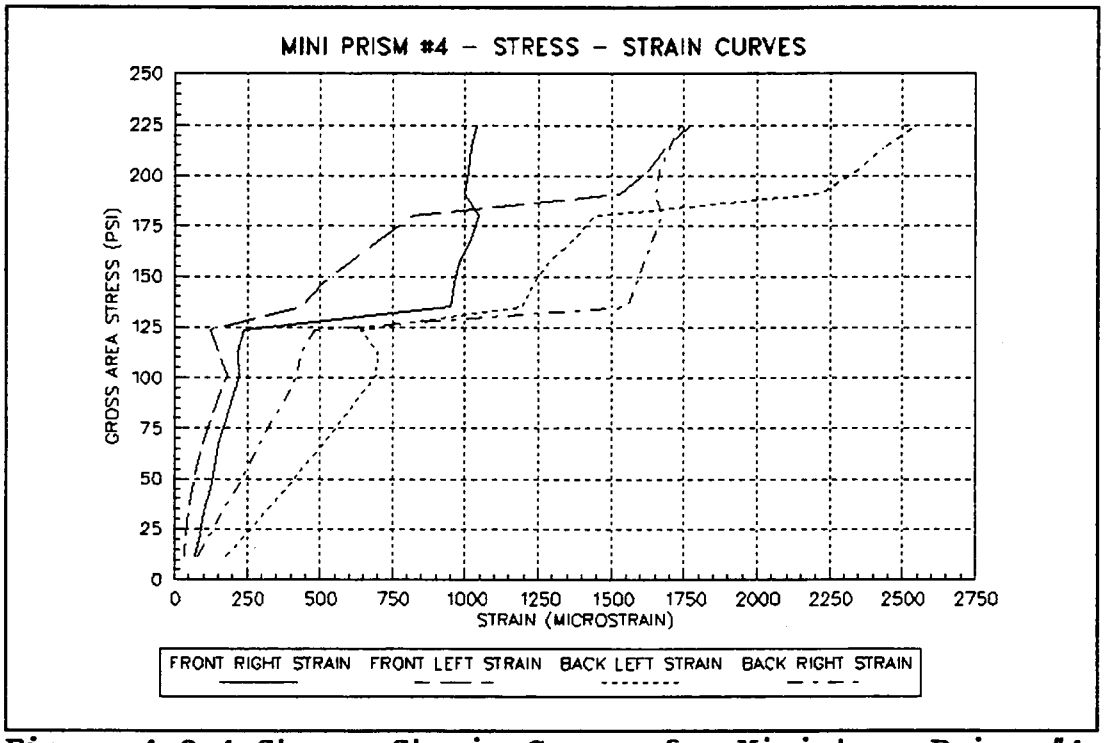


Figure 4.2.4 Stress-Strain Curves for Miniature Prism #4

strain against the gross area applied stress. The gross area for 8 inch structural clay tile was 88.90 in^2 (Flanagan et al., 1992). These stress - strain curves reflect the prism behavior up to the peak of the first loading cycle only, or to when the LVDTs were removed.

The failure modes exhibited by the miniature prisms were similar to modes reported by Boyd (1993). Boyd (1993) stated that 2' by 4' prisms with cores oriented horizontally exhibited a cracking pattern along the interior web. The miniature prisms also exhibited this behavior, with the cracks forming at the intersections of the webs as shown in figure 4.2.5. These cracks can possibly be attributed to the high stress concentrations which result from stresses being transferred along the webs. These stresses are both longitudinal stresses set up by the compressive load, as well as lateral stresses being formed in the horizontal webs due to the effect of Poisson's ratio. Similar to the larger prisms, failure occurs explosively. The faceshells are left with a high slenderness ratio after losing support from the webs. As in the tests run by Boyd, the prisms, especially the web sections, were usually reduced to rubble.

The first cracks can be tied into behavior shown in the stress strain curves. As the load increases on the prism, energy is built up in the webs of the prisms. This energy is released as the cracks form. The formation of these cracks coincide with 'jumps' in the stress strain

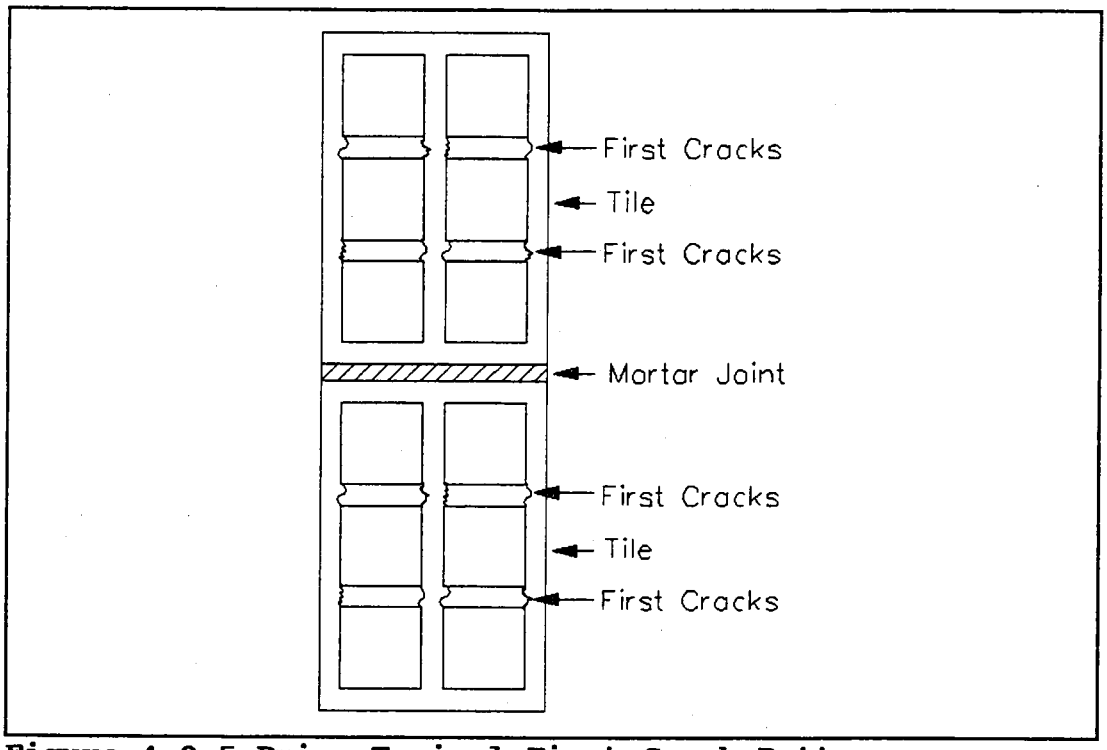


Figure 4.2.5 Prism Typical First Crack Patterns

curves. As can be seen in figures 4.2.2, 4.2.3, and 4.2.4, the curves flatten out as the strain greatly increases with little increase in the stress. Figure 4.2.1 does not display this behavior, as it is possible that the LVDTs were removed prior to the formation of the first cracks.

The tests conducted on tile coupons and mortar cylinders can also be utilized to help explain the formation of these cracks. As the load increases, both the longitudinal and lateral strains also increase in the sample. The coupon and mortar tests determined the values of Poisson's ratio, ν, and the modulus of elasticity, E, for both the tile and mortar. For the coupons in tension, the average value of E was 3,110,000 psi and the average ν was

0.141, while in compression the E value was 3,760,000 psi and ν was 0.0430. For the mortar in compression, the average E was 2,000,000 psi and the average ν was 0.155. The average values of Poisson's for the two components demonstrates how the mortar is expanding laterally much more quickly than the tile. The tile is confining this lateral expansion and thus the mortar causes horizontal tensile stresses in the tile. Using the relationship:

$$\sigma = E\epsilon$$

the approximate tensile stress of the tile at cracking can be calculated. For miniature prism #2, the cracks occur at approximately 220 psi stress and 750 longitudinal microstrain. Multiplying this strain by the average ν for the tile in tension gives a lateral strain of approximately 106 microstrain. Then multiplying this strain by the average E in tension gives a tensile stress of approximately 330 psi. This method would result in tensile stresses for prisms 3 and 4 of 175 psi and 220 psi, respectively. This results in an average value for the 4 prisms of tensile stress at cracking of 242 psi. Although this value is low, it falls within the values set forth in chapter 2 for the tensile strengths of the coupons.

The post cracking decrease in the right strain readings in figure 4.2.2 is possibly due to eccentric loading occurring in this sample, or a local failure on the right side of this sample resulting in the prism 'pinching'

MINI PRISM #	ULTIMATE LOAD, KIPS	GROSS AREA ULT. STRESS, PSI	NET AREA ULT. STRESS, PSI	GROSS AREA E, PSI	NET AREA E, PSI
1	51.4	578	2,247	720,000	2,800,000
2	33.6	378	1,469	518,000	2,010,000
3	54.8	616	2,395	481,000	1,870,000
4	40.6	457	1,774	313,000	1,210,000
AVERAGE	45.1	507	1,971	508,000	1,970,000
C.O.V.	18.8%	18.7%	18.8%	28.5%	28.7%

C.O.V. = Coefficient of Variation

Figure 4.2.6 Miniature Prisms Test Results

towards the left.

The material properties calculated for the prisms were the ultimate gross area stress, the ultimate net area stress, the gross area modulus of elasticity and the net area modulus of elasticity. All of these results, along with the ultimate loads are listed in figure 4.2.6.

The ultimate gross area stress was calculated by dividing the ultimate applied load by the gross area of the tile. As previously reported, this value is 88.90 in^2 (Flanagan et al., 1993). The ultimate net area stress was calculated by dividing the ultimate applied load by the net area with cores horizontal, with this area being 22.88 in^2 (Flanagan et al., 1993).

The gross area modulus of elasticity (E) and the net area E were calculated by using linear regression on the stress - strain data. All 4 strain readings were averaged and then plotted versus the applied gross area or net area stresses. The plot was inspected to determine the extent of the linear portion, and linear regression was performed on this linear portion. For prism 1, the linear regression was performed on the data up to 11,000 lbs applied load, or approximately 125 psi gross area stress. For prisms 2 and 3, the regression was used on the data up to 14,000 lbs applied load, or approximately 160 psi gross area stress. Finally, prism 4 had linear regression performed on the data up to 9,000 lbs applied load, or approximately 100 psi gross area stress.

The calculated stresses vary somewhat, with a coefficient of variation of approximately 18.7% for both the gross area and net area stresses. This difference could have been due to several factors. The second prism displayed a reduction in the strains on right side, and this possible eccentricity could have contributed to a premature failure. Also, initial defects in the prism could also have caused this prism to have experienced a reduced ultimate load. Prism 4 could have also had initial defects or local failures which caused a reduced load. Prisms 1 and 3 had fairly consistent ultimate loads and stresses.

4.3 Comparisons with Other Prism Tests

A prism testing program was executed at the University of Tennessee in 1992 and 1993. These tests were performed on 2′ by 4′ prisms. These prisms had differing core and bed angles (Boyd, 1993). The results in section 4.2 were compared to the horizontal cores with a bed angle of 0° from the UT tests as well as with other prism tests.

Figure 4.3.1 shows the comparisons of the current results to those of other tests. The other tests were on larger prisms. As can be seen from these results, the miniature prisms had a lower strength than the prisms tested by Boyd. Although the strengths obtained for the miniature prisms compare favorably with the results of Johnson and Matthys (1973) and Whittemore and Hathcock (1923), the real comparison should be made to Boyd's (1993) results, as the prisms were constructed of the same materials.

Boyd's prisms had greater strengths than the miniature prisms, and this could be attributed to several factors. First, the miniature prisms were two whole structural clay tiles using stack bond construction, with Boyd's prisms being both larger and using running bond construction. This difference in construction methods could account for some differences, as Boyd stated that the prisms exhibited cracks in their vertical mortar joints prior to cracks forming in the webs (Boyd, 1993). As these cracks formed in the mortar joints, load was then transferred from these joints to the

SOURCE	GROSS AREA COMPRESSIVE STRENGTH, PSI	NET AREA COMPRESSIVE STRENGTH, PSI
CURRENT RESULTS	507	1,971
BOYD, 1993	810	3,283
WHITTEMORE AND HATHCOCK 1923	393	1,795
STANG, ET AL., 1926 TILE A	360	1,587
STANG, ET AL., 1926 TILE B	230	1,012
JOHNSON AND MATTHYS 1973	629	2,200

Figure 4.3.1 Comparison of Prism Results

tiles and then to the webs. In the miniature prism tests the load was carried solely by the tiles as no vertical mortar joints were present. This absence of vertical mortar joints meant that the stress built up quicker in the web sections of the miniature prisms than in the larger prisms. This build up could have accounted for premature failures.

Secondly, the absence of running bond construction meant that no 'keying' action took place. The miniature prisms had no interaction of mortar joints and tile. This interaction can increase the load carrying capacity of the prism. This is possible because of the vertical mortar joints having mortar in the webs, with this mortar carrying load.

Third, the miniature prisms lacked the capability of transferring load. In larger prisms load transfer can occur; when one tile in a course fails, the load can be transferred to adjacent tile. In the miniature prisms, this transfer cannot take place, as no other tile is present.

The ACI 530 code specifies a correction factor for different prism height to thickness ratios. However, as the height to thickness ratio increases, so does the correction factor. For the miniature prisms the height to thickness ratio was approximately 3.0. This would result in a correction factor of 0.88 for the miniature prisms (ACI, 1992). This would mean that the strength of the miniature prisms would be reduced further. However, the code also specifies the prisms are to be built using stack bond, as were the miniature prisms. The prisms tested by Boyd used running bond, which could account for higher strengths. These and other unidentified factors could cause lower strengths than the larger prisms.

Chapter 5

TESTING PROCEDURES AND RESULTS OF BOND WRENCH SAMPLES

Introduction

This chapter analyzes the bond wrench tests which were performed. These tests were carried out in two sessions, with different testing procedures and objectives. A total of twenty five samples were tested, six samples in the first set of tests and nineteen in the second set. The first set of tests were carried out with both the ultimate load and deflections, on the tensile and compressive faces, being measured. This was done to analyze the shift of the neutral axis in these samples. The second set of tests were performed with four different types of mortar. Five bond wrench samples were built out of each type of mortar, with only the ultimate load being recorded. These tests were performed to gain insight into the effects of different mortar types on bond strength. The results of these tests are then compared to other tests which were performed by different sources.

5.1 Bond Wrench Samples Preparation and Testing

All of the bond wrench samples tested at the University of Tennessee were constructed from two 8" x 12" x 12" structural clay tiles using a stack bond with a 3/4" mortar joint. Also, all of the samples were tested using the bond

wrench illustrated in figure 5.1.1, with the bond wrench set up shown in figure 5.1.2.

The first set of bond wrench samples were constructed of type N masonry cement mortar, using 1 part type N masonry cement and 2 1/2 parts natural river sand, mixed with water. The samples were laid up using face shell and end bedding, and allowed to air dry for approximately 120 days before being tested. The samples were then put into the bond wrench apparatus as shown in figure 5.1.2. This set-up consisted of the following steps. First, a steel tube was tied to the floor using bolts and the threaded inserts which are embedded in the floor of the structural research laboratory. Next, the bond wrench sample was put next to this tube, with the sample's cores horizontal to the floor and parallel to the tube. Another steel tube was placed on the other side of the bond wrench sample, and then bar clamps were used to securely fasten the sample between these tubes. Next, the bond wrench was put over the top of the sample, and the bond wrench was tightened, via a plate and 4 bolts, onto the sample.

The bond wrench was slightly modified for these tests. In previous tests performed with this bond wrench, the center of gravity of the bond wrench and the center of gravity of the test sample did not coincide. This resulted in an additional eccentricity term having to be included in the calculation of the flexural strength of the

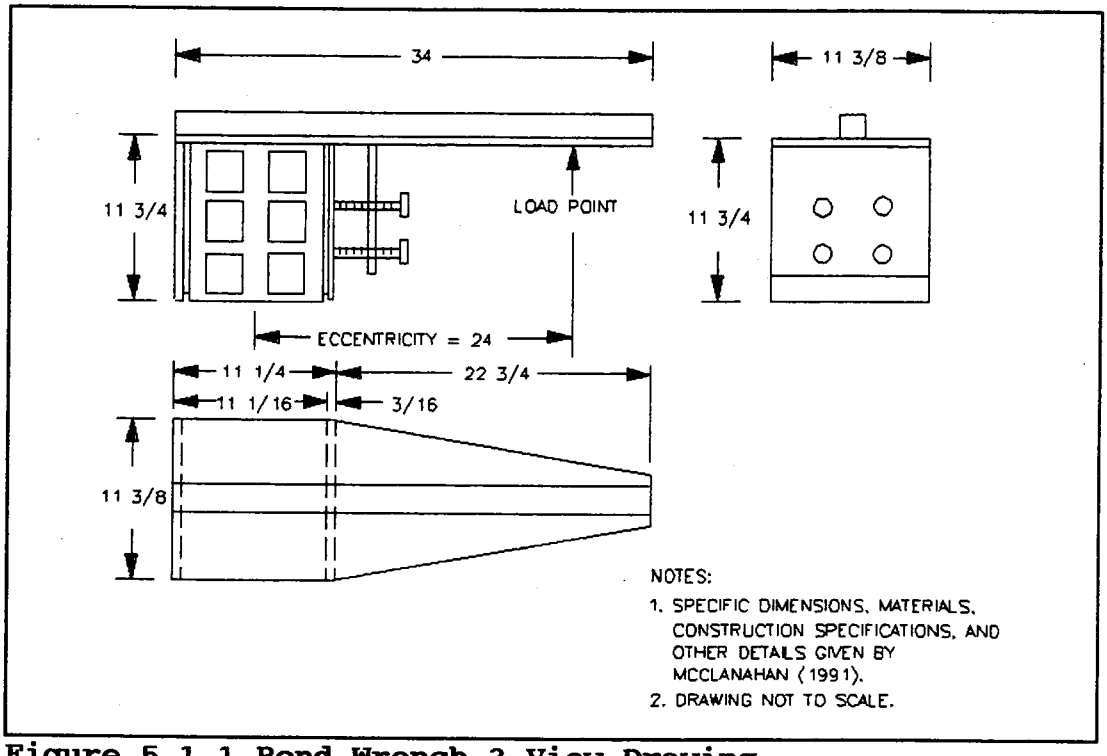


Figure 5.1.1 Bond Wrench 3 View Drawing

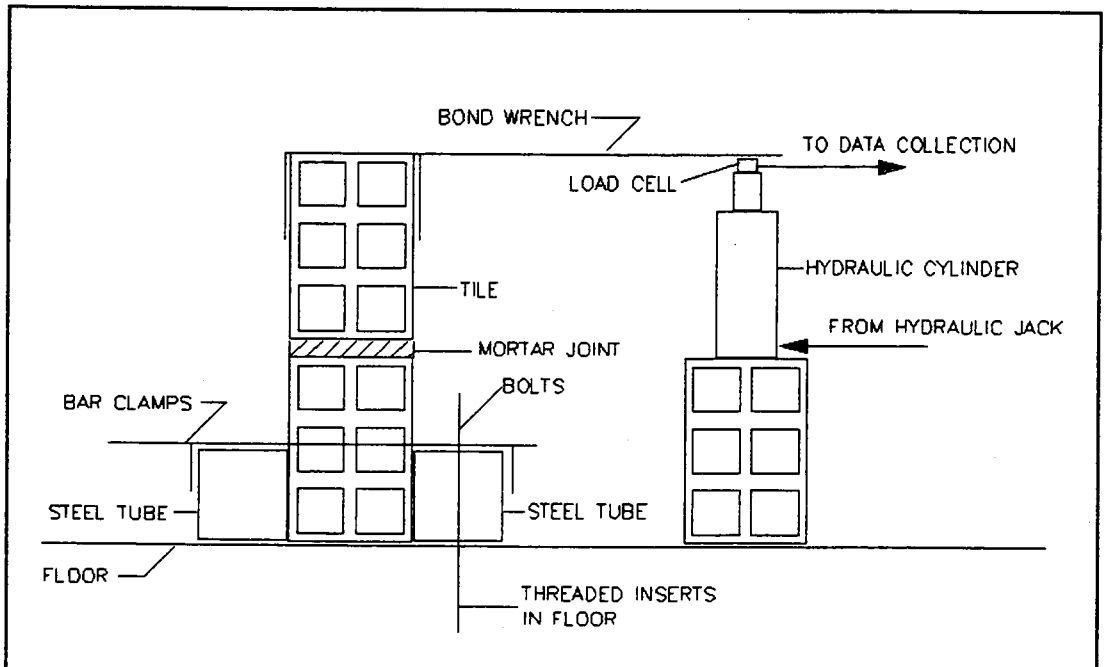


Figure 5.1.2 Bond Wrench Test Apparatus

sample, f. To avoid having to include the eccentricity term, a pry bar was inserted into the end of the bond wrench and was positioned such that the center of gravity of both the bond wrench and sample coincided. The pry bar had no effect on the ultimate load applied to the samples.

For the first set of tests, four linear variable displacement transducers (LVDTs) were attached to the bond wrench sample prior to placing the bond wrench on the sample. The attachment was accomplished using mounting brackets and angle iron stops. These brackets and stops were attached to the tile using a hot glue gun. The LVDTs were attached on the sides of the tiles at the center of the face shell and at the first cross web, on both the tensile and compressive faces.

After attaching the LVDTs, the bond wrench was attached to the sample. In these first set of tests, two different methods of loading were utilized. Sample #1 was loaded first with sand and then with a hydraulic cylinder. Samples 2 through 5 were loaded only with the hydraulic cylinder, and sample #6 was loaded only with sand. To load the samples with sand, a 5 gallon bucket had a small rectangular metal plate attached to the handle. This plate was centered over the top of the load cell which was placed on top of the bond wrench, and the bucket was filled with sand until failure. For the hydraulically loaded samples, the bond wrench was loaded using a hydraulic cylinder loaded through

a load cell onto the bottom of the bond wrench.

The LVDTs and load cell were wired into a STB 884/SCV terminal block, with the terminal block connected via 32 pin data cable, to a Megadac 3008 data collection system. The Megadac was mated via IEEE 488 interface, to an IBM PS/2 personal computer. The sampling rate was ten samples per second.

The second set of bond wrench samples were laid up using a full bed joint, and allowed to dry for twenty one days before testing. Of these twenty samples, five each were constructed using four different mortar mixes. First, type N masonry cement mortar with 1 part type N masonry cement to 2 1/2 parts natural river sand was used for five samples. Next, type S masonry cement mortar with the same proportions was used to lay up five more samples. Both of these mix proportions resulted in an aggregate to cementious material ratio of 2.50. Next type N portland cement lime (PCL) mortar was used. This mortar used 1 part portland cement, 7/8 parts mason's lime, and 4 3/4 parts natural river sand. This mixture resulted in an aggregate to cementious material ratio of 2.53. Finally, five samples were constructed using type S PCL mortar. The proportions of this mortar were 1 part portland cement, 3/8 parts mason's lime, and 3 1/2 parts natural river sand. This mixture resulted in an aggregate to cementious material ratio of 2.55. All of the mortar mixes were mixed with

enough water such that a workable mortar was achieved.

These samples were put into the bond wrench in the same manner as the first set of samples, with the exception that these samples had no LVDTs attached. These samples were also tested using the modified bond wrench which was previously mentioned. All of these samples were loaded using the hydraulic jack. The data collection used for these samples was the same as that used for the first set of samples, with the exception that only load readings were taken.

5.2 Bond Wrench Test Results

The first set of bond wrench samples were tested and the data was used to construct load deflection curves, as well as to calculate the flexural strength of the sample, f.

The load deflection curves were constructed to show that the tensile deflections were much greater than the compressive deflections. These curves are shown in figures 5.2.1, 5.2.2, 5.2.3, and 5.2.4. All of the curves reflect the data obtained during the hydraulic loading only. The curves obtained using the sand loaded portions were extremely erratic and considered inaccurate.

As can be seen in the curves, the tensile deflections are much greater than the compressive deflections. This could be due to two possible reasons. First, the modulus of elasticity in tension is probably different than the

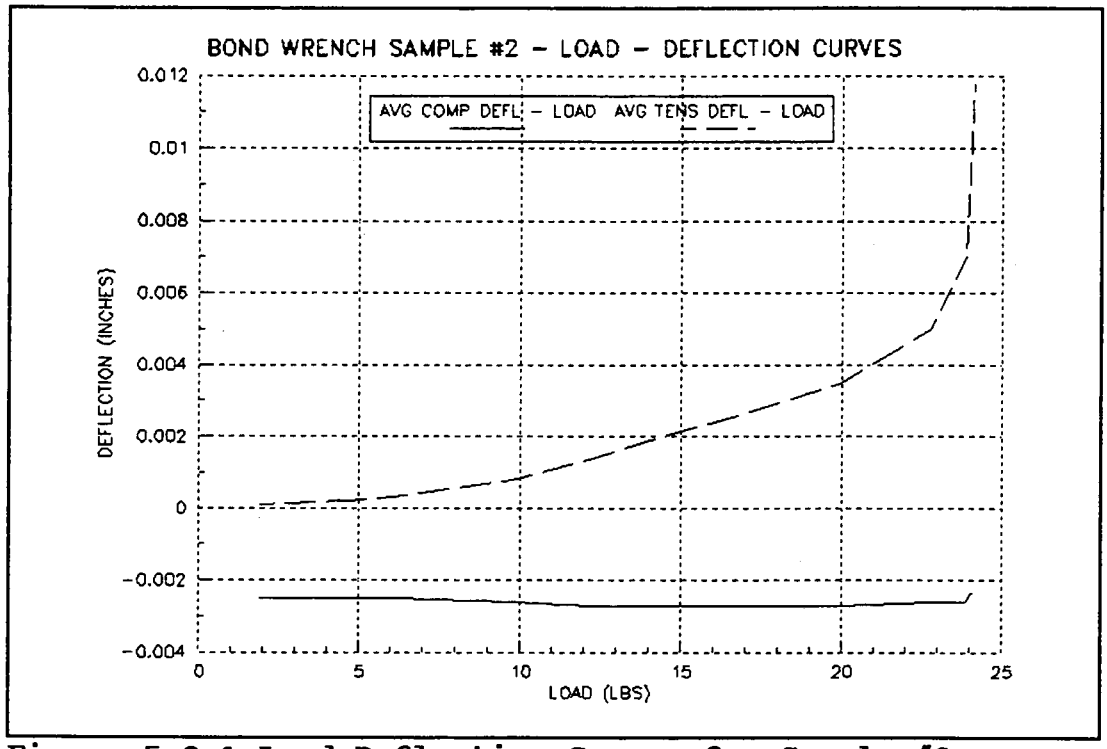


Figure 5.2.1 Load Deflection Curves for Sample #2

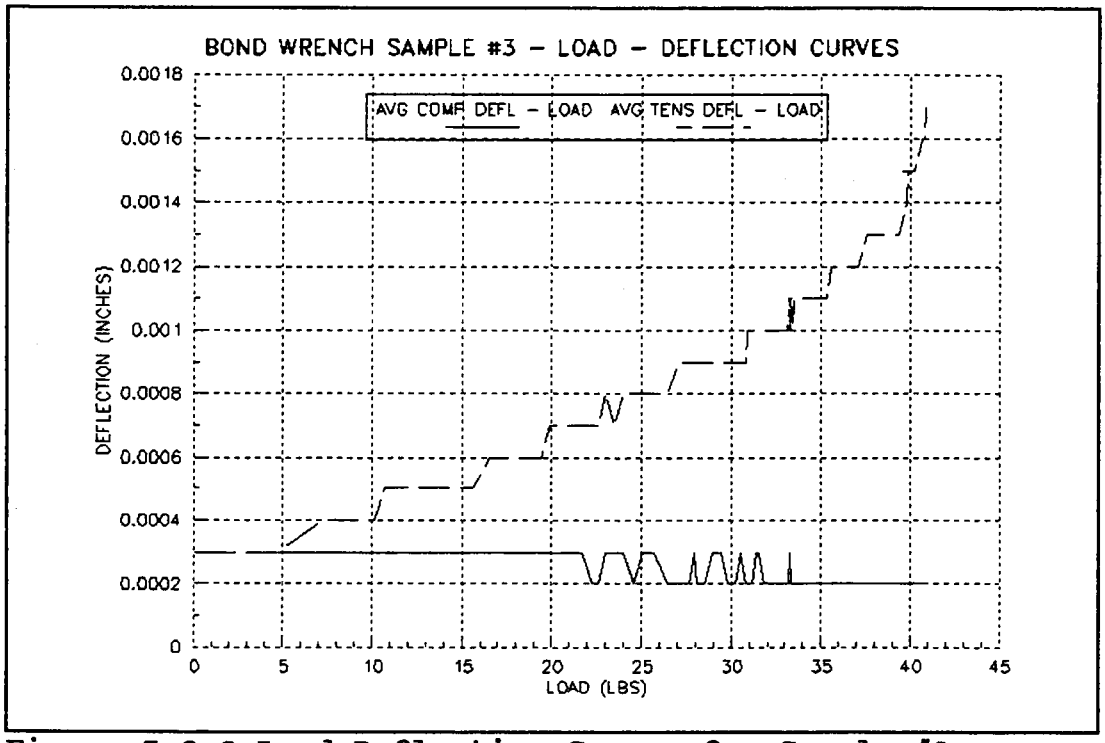


Figure 5.2.2 Load Deflection Curves for Sample #3

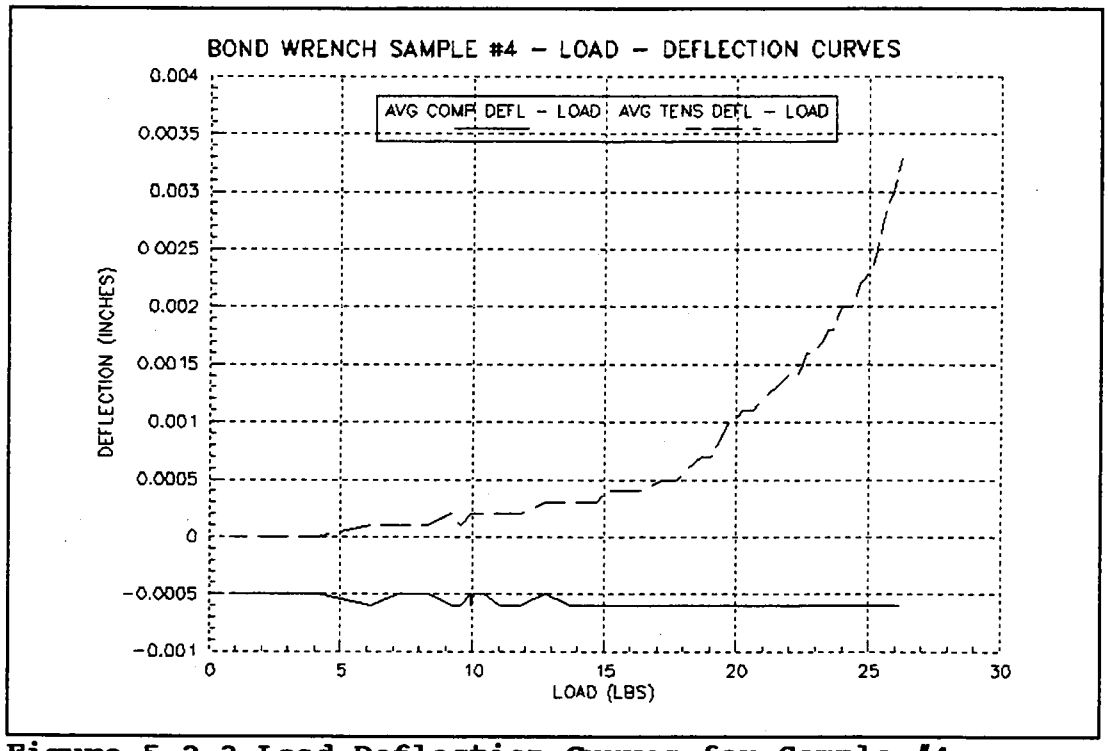


Figure 5.2.3 Load Deflection Curves for Sample #4

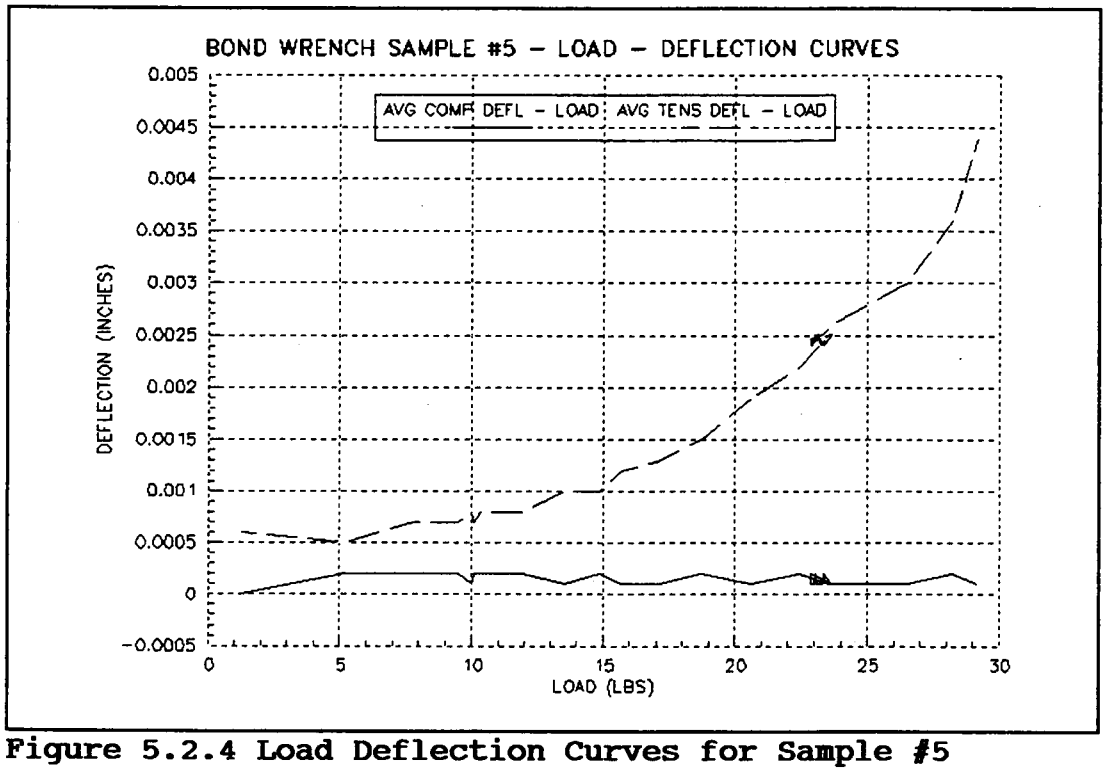


Figure 5.2.4 Load Deflection Curves for Sample #5

modulus of elasticity in compression. Because the tensile deflections were significantly higher than the compressive deflections, different moduli of elasticity should be assigned to the tensile and compressive faces (Fried, 1992). Second, the shifting of the neutral axis could also partially explain the tensile deflections both being greater and also increasing at a much higher rate. Using simple bending theory, when the bed joint between two masonry units is loaded eccentrically, the neutral axis should shift towards the tensile face (Fried, 1992). However, work done by Anderson and Held has shown that the neutral axis shifts toward the compression face when the bed joint is subjected to an eccentric load (Anderson and Held, 1983). Their explanation of this behavior is that the stiffness in the tensile zone of the sample is less than the stiffness in the compression zone. Once again, this difference in stiffness would account for both greater deflections and a higher rate of increase occurring in the tensile zone.

The calculation of the flexural strength of the samples was accomplished using the following formula:

$$f = \frac{6\,(PL - P_1L_1)}{bd^2} + \frac{(P - P_1)}{bd}$$

Where:

f = Flexural tensile strength, PSI

P = Maximum applied load, lbs

P_1 = Weight of bond wrench and tile, lbs

L = Distance from center of bond wrench sample to loading point, in.

L_1 = Distance from center of bond wrench sample to centroid of bond wrench, in.

b = Average length of cross section of bond surface, in.

d = Average width of cross section of bond surface, in.

The values determined for the first set of tests were as follows:

f = listed in figure 5.2.5

P = listed in figure 5.2.5

P_1 = 101.97 lbs

L = 24 in.

L_1 = 0 in.

b = 11.54 in.

d = 7.67 in.

The results of the calculations of f are listed in figure 5.2.5, along with the ultimate loads. As can be expected in this type of testing, a high amount of variability is present in these samples. Tests conducted by Martin Marietta Energy Systems also yielded a high amount of variability (MMES, 1992). This variability is explored further in the next section when comparisons to other results are presented.

The second set of samples were tested with only the

Test #	Ultimate load, lbs.	f psi
1	92.7	19.55
2	24.2	4.24
3	40.8	7.97
4	26.2	4.70
5	29.2	5.37
6	36.4	6.97
Averages	41.6	8.13

Coefficient of Variation of f = 64.8%

Figure 5.2.5 Flexural Strengths of First Set of Samples

ultimate load being recorded. This set of tests were conducted to find correlation between mortar type and flexural strength, f. The results of these tests are shown in figure 5.2.6.

The calculation of the flexural strengths of the samples was made with the same formula used in the first set of samples, with the variables also remaining the same. As can be seen in figure 5.2.6, a moderate degree of variability exists in the results. Possible explanations of the variability are that in the type N masonry cement samples, one sample broke in handling, thus limiting the number of samples to four. Second, the lowest values of f in both the type N PCL samples and type S PCL samples

	Type N Masonry Cement Mortar	Type S Masonry Cement Mortar	Type N PCL Mortar	Type S PCL Mortar	Overall Results
# of Tests	4	5	5	5	19
Avg. Load, lbs.	71.0	92.6	117.8	113.2	100.2
Avg. f, psi	14.72	19.54	25.16	24.22	21.23
C.O.V.	47.3%	20.9%	17.2%	26.2%	31.7%

C.O.V. = Coefficient of Variation

Figure 5.2.6 Flexural Strengths of Second Set of Samples

occurred in samples having voids in the center of their bed joints. Third, a high degree of variability exists in this type of testing.

The type N masonry cement samples displayed an average value of f of 14.72 psi. In the first set of tests the average value of f was 8.13 psi. Possible explanations of these differences could be sample age, mortar strengths, possible jarring of the samples in handling, and construction differences.

Sample age could account for some differences. It is usually assumed that as the sample ages the flexural strength of the joint increases. However, some previous work has shown that the highest strengths occur as early as

three to seven days after building (Baker, 1979). The first set of samples aged for approximately 120 days before testing and the second set aged for twenty one days.

Mortar strengths could also account for some differences in the flexural strengths of the different sets. However, no mortar cubes were tested for the first set of samples. The cube strengths, at a mortar age of fourteen days, for the second set of samples are listed in figure 5.2.7.

Possible jarring of the samples could also account for differences in the results. The first set of samples were built in a separate room and then moved into the lab for testing. The second set of samples were built in the lab and only had to be moved into the bond wrench.

Finally, construction practices could also account for some difference in the test results. The first set of samples was constructed using face shell and end bedding. This resulted in a bed joint around the edges of the sample. The second set of samples was constructed using a full bed joint. This full bed joint could add some strength to the sample as the area of stress is increased.

The difference between the type N masonry cement and type S masonry cement samples were as expected. The type S masonry cement mortar had a fourteen day strength of 1967 psi, while the type N masonry cement mortar had a fourteen day strength of 1358 psi. The type S mortar displayed

	Masonry Cement Mortar		Portland Cement Lime Mortar	
	Type N	Type S	Type N	Type S
	Ultimate Stress, psi	Ultimate Stress, psi	Ultimate Stress, psi	Ultimate Stress, psi
Cube #1	1325	2025	975	1700
Cube #2	1425	2025	1025	1975
Cube #3	1325	1850	900	1300
Average	1358	1967	967	1658
C.O.V.	3.5%	4.2%	5.3%	16.7%

C.O.V. = Coefficient of Variation

Figure 5.2.7 Comparison of Mortar Cube Strengths

higher flexural strengths as well. The higher compressive strength mortar should also form a higher strength bond to the tile.

The type N PCL mortar and type S PCL mortar samples both had higher flexural strengths than both the masonry cement mortar samples. This is expected because of the higher lime content in the PCL mortars. Lime increases bond strength, which is why the results of type N PCL mortar samples versus type S PCL mortar samples are surprising. Type N PCL samples displayed higher flexural strengths than the type S PCL samples. The type N PCL mortar had a fourteen day compressive strength of 967 psi while the type S PCL mortar had a fourteen day strength of 1658 psi. These

results show that flexural strength probably depends more on lime content than mortar strength. Type N PCL mortar samples had a lime content of 13.2%, while the type S PCL mortar samples had a lime content of 7.7%. Although the difference in average flexural strengths is slight, 25.16 psi for type N PCL and 24.22 psi for type S PCL, the difference in lime contents and mortar compressive strengths show how lime content effects the flexural strength.

All of the cubes displayed fairly consistent results, with low coefficients of variation. All of the strengths are compared in figure 5.2.7.

5.3 Comparisons with Other Test Results

In this section, the results of other bond wrench tests are compared to the results reported in the previous section. Figure 5.3.1 shows the differences in the flexural strengths of the other tests. Although these other tests used different equipment, mortar types, and construction practices, relationships can still be defined.

The closest correlation can be drawn between both UT tests and McClanahan's results. The same bond wrench and set up was used in all three tests. McClanahan also used stack bond construction as well as face shell bedding. However, he did not modify the bond wrench so that the center of gravity of both the bond wrench and tile coincided. This resulted in a L_1 value not being zero.

Source	UT 12/23/92	UT 3/15/94	McClanahan	MMES
# of Tests	6	19	7	25
Avg. Load, lbs.	41.6	100.2	109.3	59.6
Avg. f, psi	8.13	21.23	19.72	9.57
C.O.V.	64.8%	32.0%	36.8%	60.0%

C.O.V. = Coefficient of Variation

Figure 5.3.1 Comparison of Different Bond Wrench Tests

Also, he did not use the same values of b, d and P_1 as the UT tests did. He used 11.625 in. for b, 7.75 in. for d, and 87.5 lbs. for P_1. However, the different values of b and d would not significantly affect the results. Also, the difference in P_1 would not affect the results.

The mortar used in McClanahan's samples was Sakrete brand mortar mix (McClanahan, 1991). This mortar was not tested compressively, but from the average value of McClanahan's flexural strengths, it is assumed that the mortar was probably type S. Also, McClanahan's samples aged for forty three days prior to testing. A deliberate attempt was made to vary the parameters in his tests, as both the tiles and mortar mix were made dry or wet. This partly

accounts for the higher standard deviation found in McClanahan's results. However, his results compare favorably with the UT tests run on 3/15/94. The 3/15/94 UT tests include all 19 samples, with 4 different mortar types used on these samples. When McClanahan's results are directly compared to UT 3/15/94 type S masonry cement mortar samples, an even closer relationship is found. McClananhan reported an average f of 19.72 psi, with a standard deviation of 7.26 (McClanahan, 1991). UT 3/15/94 type S masonry cement mortar samples had an average f of 19.54 psi with a standard deviation of 4.09.

The Martin Marietta Energy Systems (MMES) results were in situ tests run on an existing wall. This wall had previously been tested with an airbag, and the resulting flexural strengths could have been lowered by damage caused by the airbag (MMES, 1992). The wall was constructed using the same type of structural clay tile used in both UT tests as well as McClanahan's tests. This wall was constructed using a running bond. To test the flexural strengths of the tile, the course of tile above the tile to be tested was removed, being careful not to affect the lower courses. Next, the head joints were sawed so that the tile was removed from the adjoining tiles. Following this, the bed joint was carefully sawed so that adjoining tiles were separated. The bond wrench was then attached and a hydraulic cylinder was used to fail the samples. All of the

variables for these tests were comparable to the variables used in the UT tests. with the exception that each tile was measured in MMES testing, with average values utilized in both the UT tests as well as McClanahan's tests.

The results from the MMES tests compare favorably to the UT tests run on 12/23/92. The MMES results were an average f value of 9.56 with a standard deviation of 5.71. The 12/23/92 UT tests had an average f value of 8.13 with a standard deviation of 5.27. Although the MMES tests were conducted on in situ samples using running bond, a comparison to the stack bonded UT samples can be drawn. Both sets of tests displayed moderate variability.

From comparing the UT samples to previous tests, several conclusions can be drawn. First, the type of mortar appears to have an effect on flexural strength. Higher compressive strength appears to result in higher flexural strength. According to ASTM C270 , bond strength is increased both by increased compressive strength as well as water retentivity (ASTM, 1991). The addition of lime improves the mortar's water retentivity, so the use of type S mortar and PCL mortars should improve flexural strength. Second, aging of the samples appears to possibly decrease flexural strength. Also, all of the tests displayed moderate degrees of variability. In this type of testing, variability is expected, although the UT samples tested on 3/15/94 did not display quite as high a variance. Once

again, according to ASTM, bond is considered the most important single property of hardened mortar. Unfortunately, it is also the most inconsistent and unpredictable (ASTM, 1991). Finally, in situ test results appear to not vary significantly from laboratory samples.

Chapter 6

CONCLUSIONS

This research, aimed at achieving a better understanding of both the component and composite behavior of clay tile and mortar, involved four major groups of tests. Two of these tests measured component behavior, while the other two appraised composite behavior.

The clay tile coupons were evaluated using compression, tension, modulus of rupture, and absorption tests. The compression tests yielded stress - strain curves which were fairly linear up to approximately 60% of the ultimate stress. The average compressive strength was 9150 psi, with an average modulus of elasticity of 3,760,000 psi and an average Poisson's ratio value of 0.043. All of the calculated material properties, with the exception of Poisson's ratio, had coefficients of variation less than 6.7%. As seen later in the miniature prism tests, the low Poisson's value adds to the tile's tensile stresses when loaded as a prism. The tensile samples displayed very brittle behavior, much as concrete does in tension. The tensile strengths varied widely, but the stress - strain curves constructed from these tests did yield consistent behavior, remaining fairly linear up to the ultimate load. The average tensile strength was 618 psi, the average E was 3,110,00 psi, and the average ν was 0.141. The modulus of

rupture tests yielded very consistent results, with all values falling within expected bounds. The average M_r was 1,540 psi. The absorption tests yielded results very close to those requiring wetting prior to placement.

Mortar cylinders were tested in both compressive and split cylinder modes. The compressive cylinders had fairly linear behavior up to approximately 50% of the ultimate stress, and material properties were calculated for this portion of the stress - strain curves. The average compressive strength came out to 3,050 psi with an average E of 2,000,000 psi and an average ν of 0.155. The cyclic loading performed on the cylinders showed how the cylinders did display linear behavior, especially in the longitudinal or axial direction. The reload modulus was calculated for the two reload portions, and only varied by an average of 13.3%. The behavior observed in the mortar cylinder tests demonstrated how the mortar is the "weak link" in clay tile - mortar interaction. Also, a test was conducted which showed that air cured mortar tends to be stronger than moist cured mortar.

A total of 4 miniature prisms were tested in compression. Cracks formed in the webs, with these cracks separating the faceshells from the webs, leading to explosive failures. The ultimate stresses obtained by the prisms averaged 1,971 psi net area ultimate stress and an average net area E of 1,970,000 psi. Because the mortar

deforms both more quickly and more evenly than the tile, additional lateral stresses are introduced in the tile, as the tile is attempting to confine this expansion by the mortar. This confinement, in addition to the lateral stresses caused by the compressive loading, leads to the formation of cracks. The strengths obtained in these results tended to be lower than strengths obtained in tests of larger (2' x 4') prisms. The lower strengths may be because of the lack of keying action which is present in larger, running bond prisms. Also the lack of vertical mortar joints may also lead to premature failure of the miniature prisms.

The bond wrench testing showed a shift of the neutral axis towards the compression face of the samples. This can be explained in the difference in the stiffnesses of the tensile and compressive faces. The bond wrench testing also showed that both higher compressive strength and higher lime content improves bond strength. Comparisons of these results with other tests were favorable, with all of the tests displaying a moderate degree of variance.

Overall, the tests performed lead to several conclusions. First, the clay tile tends to behave much as concrete does, being strong in compression and brittle in tension, with a low value of Poisson's ratio in compression. Second, mortar is weaker in compression and has a higher value of Poisson's ratio in compression, and this allows the

mortar to deform more quickly than the tile. Third, in the compressive interaction of the mortar and tile, the tile tends to confine the expansion of the mortar, leading to possible premature tensile failure of the tile. Fourth, in bond wrench samples, contrary to the expectations of bending theory, the neutral axis shifts towards the compressive face. Finally, increasing both the compressive strength and lime content of mortar helps to raise the flexural strength.

BIBLIOGRAPHY

BIBLIOGRAPHY

American Concrete Institute, American Society of Civil Engineers, and The Masonry Society (1992). Specifications for Masonry Structures (ACI 530.1-92/ASCE 6-92/TMS 402-92). New York, New York.

American Society for the Testing of Materials. 1991 Annual Book of ASTM Standards. Section 4, Volume 4.05 Philadelphia, Penn.

Baker, L. R. (1979). "Measurement of the Flexural Bond Strength of Masonry." Proceedings of the Fifth International Brick and Block Masonry Conference. pp. 41-43.

Baker, L. R. (1979). "Some Factors Affecting the Bond Strength of Brickwork." Proceedings of the Fifth International Brick and Block Masonry Conference. pp. 41-46.

Boyd, Kurt A. (1993). "Compressive Strength and Constitutive Behavior of Clay Tile Prisms." Master Thesis. University of Tennessee, Knoxville, Tennessee

Flanagan, R. D., Bennett, R. M., and Butala, M. B. (1993). "Properties of Structural Clay Load-Bearing Wall Tile." Proceedings of the Sixth North American Masonry Conference, Volume 1, pp. 87-98.

Fried, Anton, Anderson, Colin, and Smith, David (1988). "Predicting the Transverse Lateral Strength of Masonry Walls." Proceedings of the Eighth International Brick and Block Masonry Conference. pp. 1171-1183.

Fried, Anton (1992). "The Position of the Neutral Axis in Masonry Joints." Extended Abstract at The Third International Masonry Conference.

Gere, James M., and Timoshenko, Stephen P. (1990). Mechanics of Materials. Third Edition. Boston, Mass.

Hardin, E. J. (1991). "Bond Wrench Testing at Building 9207 at the Y-12 Plant." Technical Report Y/EN-4592, Martin Marietta Energy Systems, Inc., Oak Ridge, Tennessee.

Hardin, E. J., and Wynn, C. C. (1992). "Test Procedure for Measurement of Masonry Flexural Bond Strength." Technical Report Y/EN-4602, Martin Marietta Energy Systems, Inc., Oak Ridge, Tennessee

Johnson, F. B., and Matthys, J. H. (1973). "Structural Strength of Hollow Clay Tile Assemblages." Journal of the Structural Division, ASCE, 99(ST2), pp. 259-275.

McClanahan, Sonny (1991). "Bond Wrench Report." Special Problem in Civil Engineering. University of Tennessee, Knoxville, Tennessee.

Mehta, P. Kumar (1986). Concrete Structure, Properties, and Materials. First Edition. Englewood Cliffs, New Jersey.

Miltenberger, Matthew A., Colville, James, and Wolde-Tinsae, Amde M. (1993). "Relationship Between Cube and Cylinder Compressive Strength of Mortar." Proceedings of the Sixth North American Masonry Conference, Volume 2, pp. 1025-1036.

Park, R. and Paulay, T. (1975). Reinforced Concrete Structures. First Edition. New York, New York.

Plummer, Harry C. (1962). Brick and Tile Engineering. Second Edition. McLean, Virginia.

Southern Building Code Congress International, Inc. (1991). 1991 Standard Buliding Code. Birmingham, Alabama.

Stang, A. H., Parsons, D. E., and Foster, H. D. (1926). "Compressive and Transverse Strength of Hollow - Tile Walls." National Bureau of Standards Technologic Paper 311, Volume 20, pp. 317-353.

Whittemore, H. L., and Hathcock, B. D. (1923). "Some Compressive Tests of Hollow - Tile Walls." U.S. Bureau of Standards Technologic Paper No. 238, Volume 17, pp. 513-527.

APPENDIX

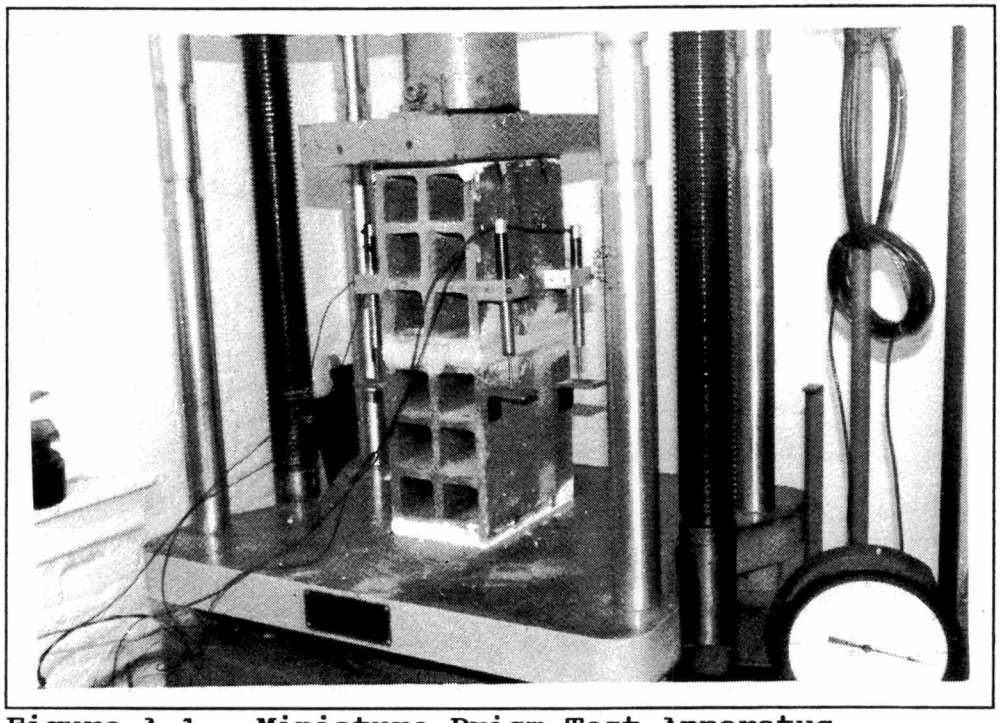


Figure A.1 - Miniature Prism Test Apparatus

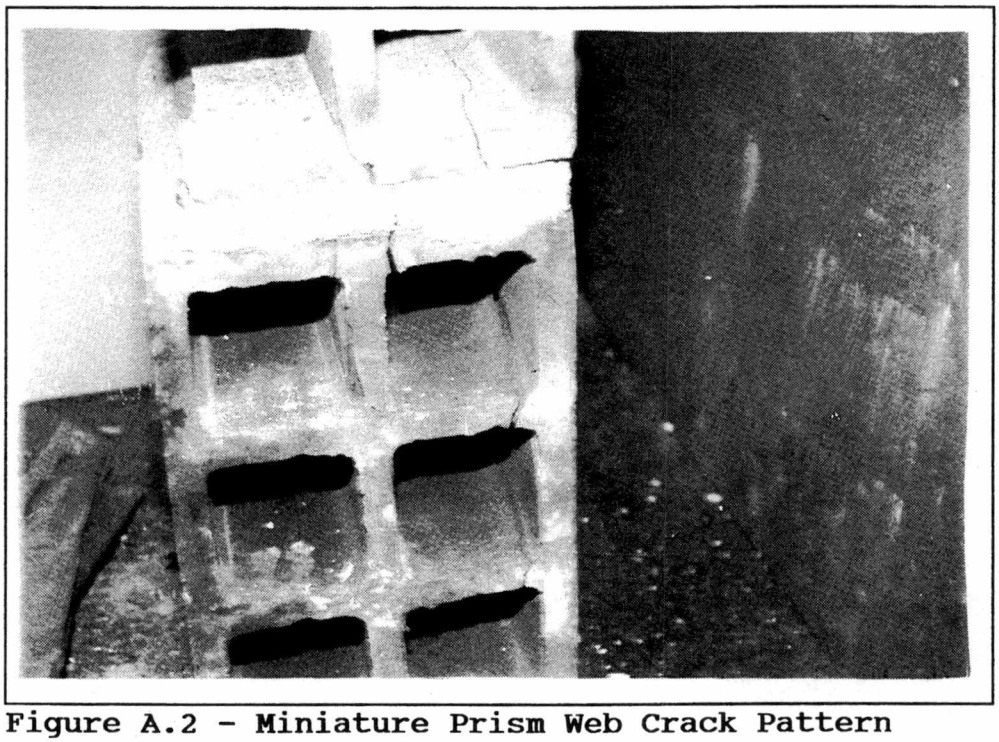


Figure A.2 - Miniature Prism Web Crack Pattern

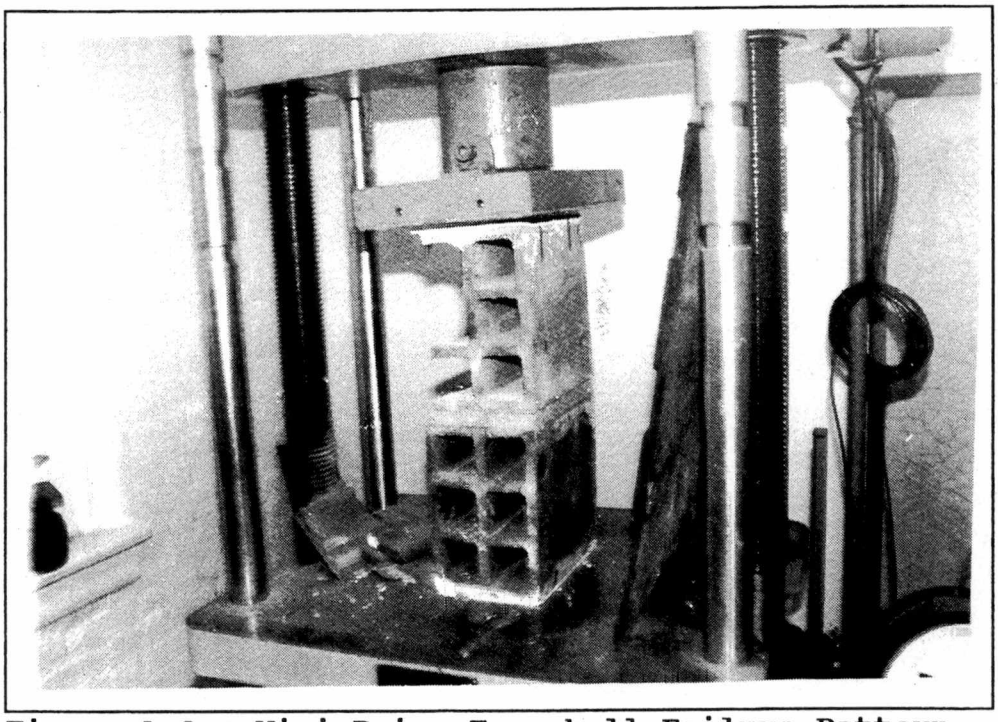


Figure A.3 - Mini Prism Faceshell Failure Pattern



Figure A.4 Mini Prism Explosive Failure Pattern

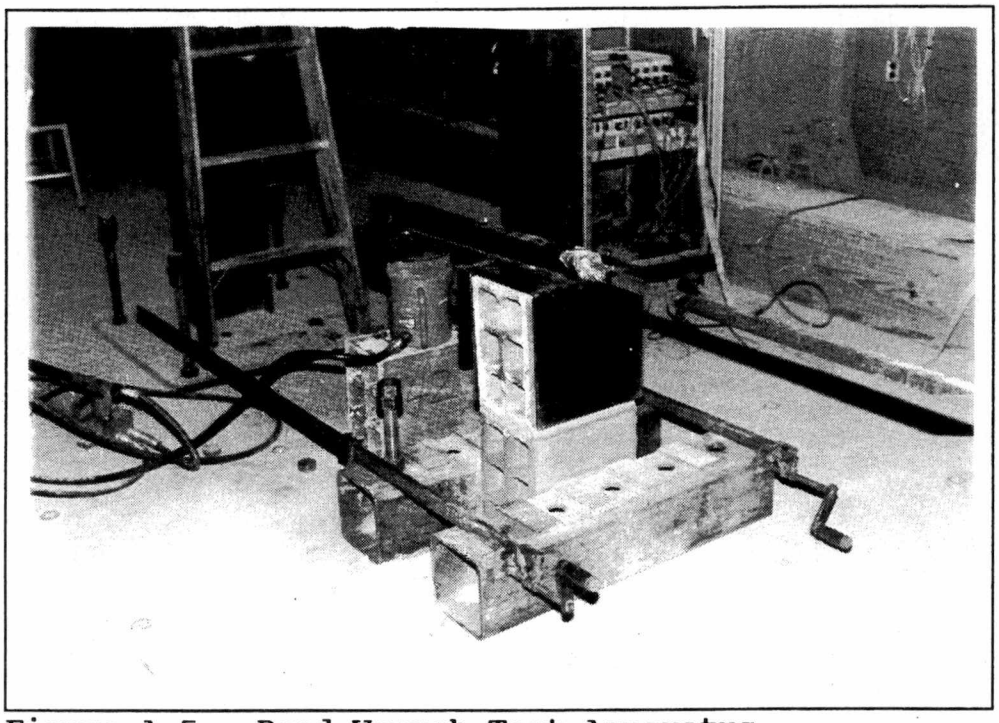


Figure A.5 - Bond Wrench Test Apparatus

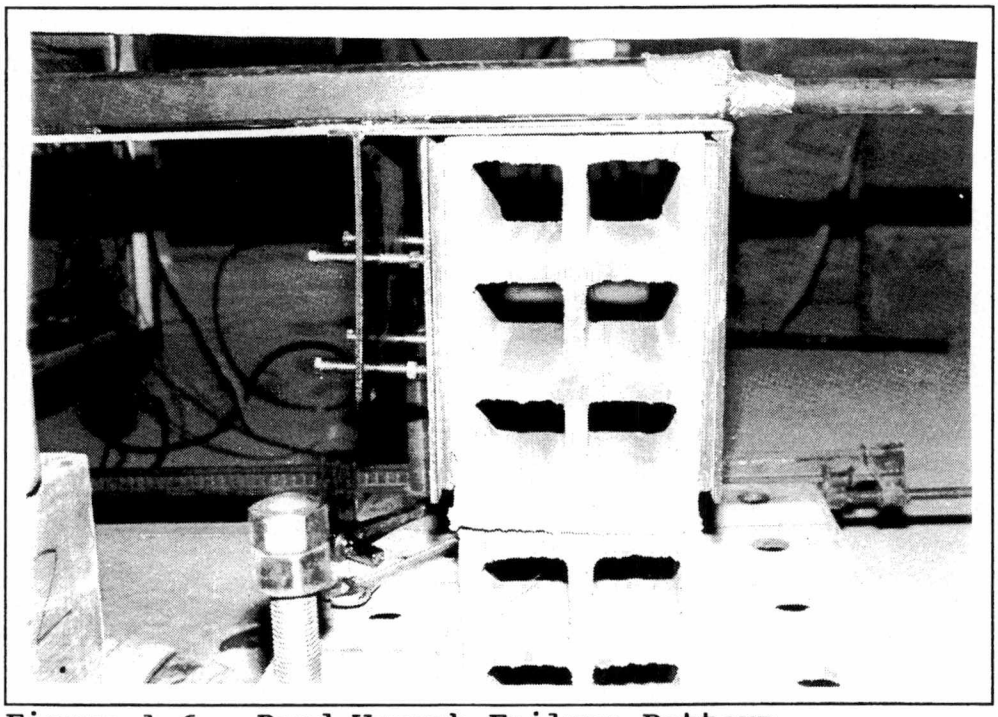


Figure A.6 - Bond Wrench Failure Pattern

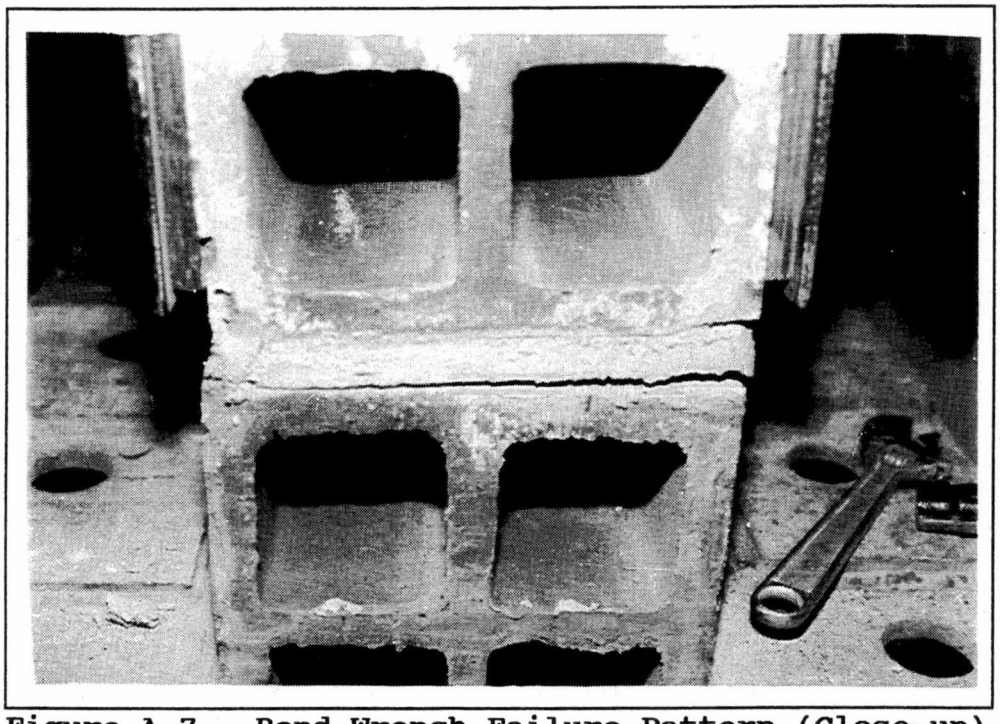


Figure A.7 - Bond Wrench Failure Pattern (Close-up)

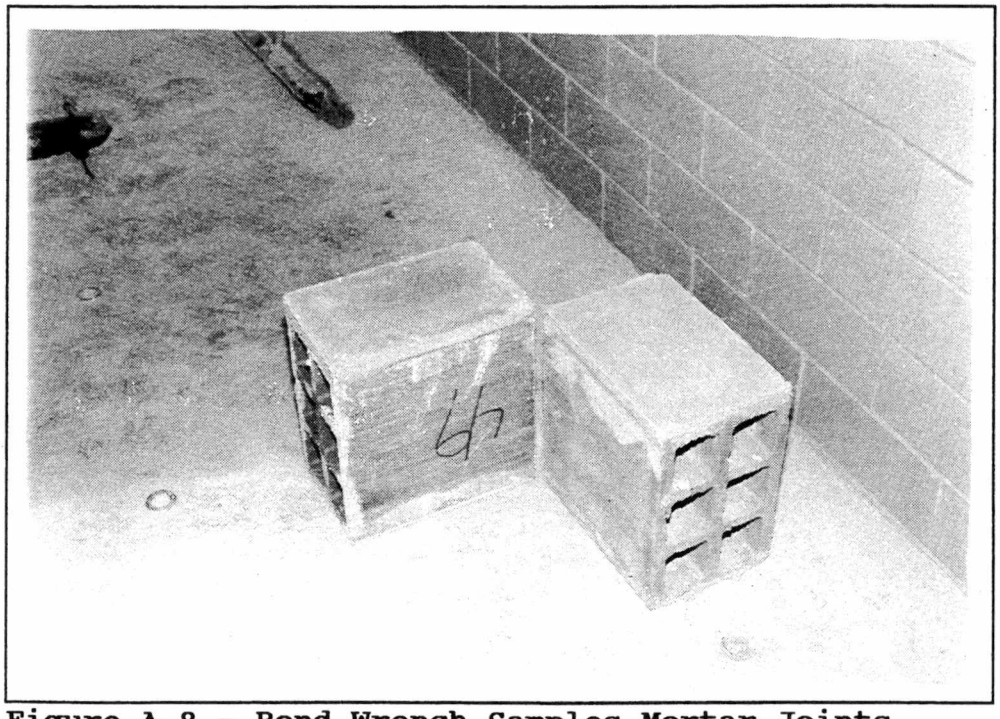


Figure A.8 - Bond Wrench Samples Mortar Joints

VITA

Christopher Eugene Columber was born August 20, 1963 in Knoxville, Tennessee. He attended Fulton High School in Knoxville, and graduated in June of 1981. Later that year, he entered The University of Tennessee - Knoxville in the School of Engineering. After attending for 1 year, he left school to work for a period of several years. In the spring of 1989 he returned to The University of Tennessee - Knoxville, again in the School of Engineering. He received a B.S. degree in Civil Engineering in December of 1992. In May of 1994, he received a M.S. degree in Civil Engineering.